Publisher version: https://doi.org/10.1016/j.ejmech.2023.115636

Coumarins as Factor XIIa Inhibitors: Potency and Selectivity Improvements Using a Fragment-based Strategy

Clara Davoine[a,b], Amandine Traina[a], Jonathan Evrard[a], Steve Lanners[a], Marianne Fillet[b,†], Lionel Pochet[a,†,*]

[a]*Namur Medicine & Drug Innovation Center (NAMEDIC – NARILIS), University of Namur, Rue de Bruxelles 61, 5000 Namur, Belgium*

[b]*Laboratory for the Analysis of Medicines (LAM), Department of Pharmacy, CIRM, University of Liege, Place du 20 Août 7, 4000 Liège, Belgium*

[†] equally contributed to the work

**Corresponding author. E-mail address:* lionel.pochet@unamur.be.

Postal address: Rue de Bruxelles 61, 5000 Namur, Belgium

Abstract

Previously, we described weak coumarin inhibitors of factor XIIa, a promising target for artificial surface-induced thrombosis and various inflammatory diseases. In this work, we used fragment-based drug discovery approach to improve our coumarin series. First, we screened about 200 fragments for the S1 pocket. The S1 pocket of trypsin-like serine proteases, such as factor XIIa, is highly conserved and is known to drive a major part of the association energy. From the screening, we selected fragments displaying a micromolar activity and studied their selectivity on other serine proteases. Then, these fragments were merged to our coumarin templates, leading to the generation of nanomolar inhibitors. The mechanism of inhibition was further studied by mass spectrometry demonstrating the covalent binding through the formation of an acyl enzyme complex. The most potent compound was tested in plasma to evaluate its stability and efficacy on coagulation assays. It exhibited a plasmatic half-life of 1.9 h and a good selectivity for the intrinsic coagulation pathway over the extrinsic one.

Publisher version: https://doi.org/10.1016/j.ejmech.2023.115636

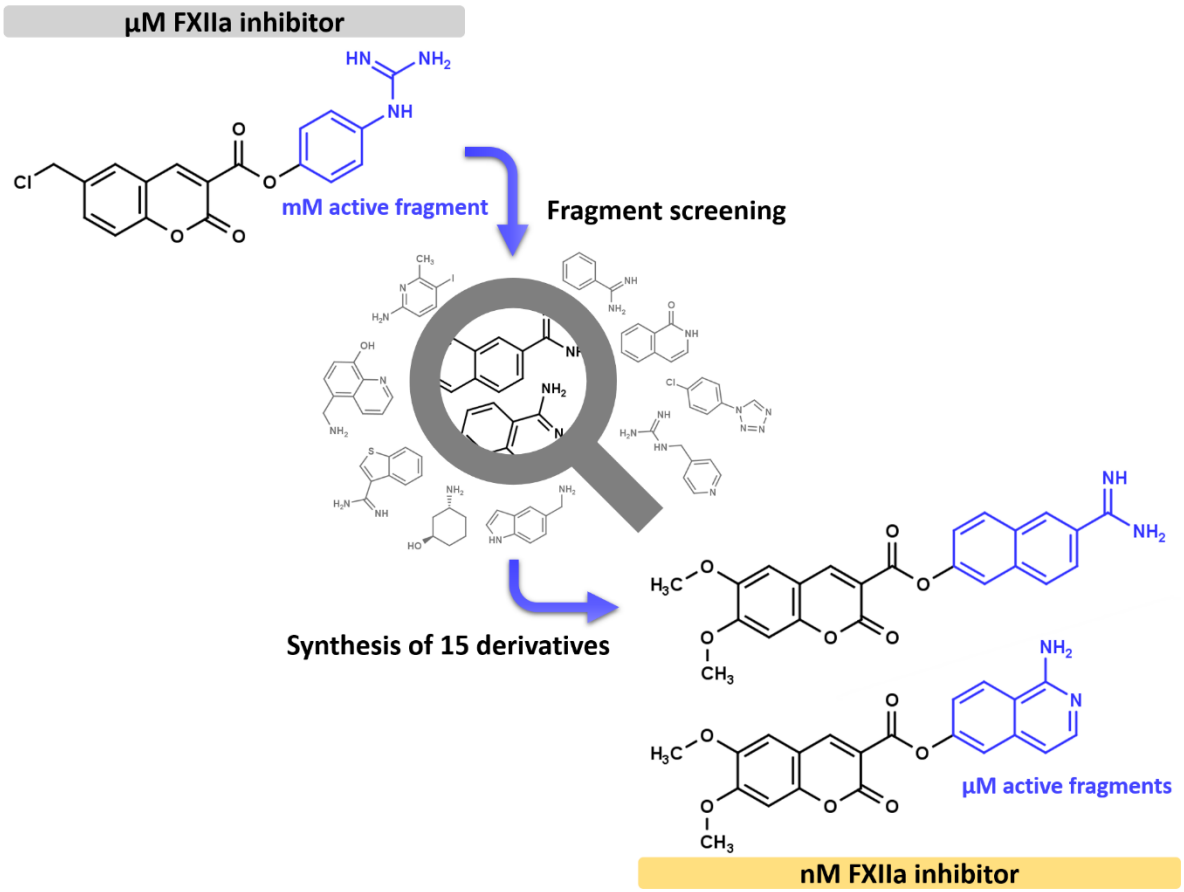

Keywords

Fragment-based drug discovery; serine proteinase inhibitors; coumarin; biochemical assay; factor XIIa; medical device-induced thrombosis.

Abbreviations

BZM, benzamidine; FXII(a), (activated) factor XII; FBDD, fragment-based drug discovery; LE, ligand efficiency; PABZM, *p*-aminobenzamidine.

Introduction

Cardiovascular diseases and cancers are the leading causes of death worldwide.[1] The treatment of cardiovascular diseases widely uses blood-contacting devices. Heart surgeries also involve the use of extracorporeal circuits. In cancer patients, venous access and drug delivery strongly rely on indwelling medical devices.[2,3] Overall, millions of these devices are employed every year and their common cause of failure is thrombus formation.[3] Contrary to healthy endothelium, synthetic biomaterials do not actively resist thrombosis and trigger clotting through a complex series of interconnected mechanisms.[3,4] Despite improvements in their blood-compatibility, systemic administration of anticoagulants (such as heparin and warfarin), antiplatelet agents, or both is needed to mitigate the thrombotic risk induced by blood-contacting devices.[2–4] However, these therapies are not systematically effective and are associated with an increased bleeding risk of the patient.[3]

In this context, FXIIa inhibition rises as a promising strategy to prevent medical device-induced thrombosis more safely than the current pharmacotherapies. Indeed, FXII adsorption and autoactivation on artificial surfaces are the initial events leading to contact-mediated thrombosis induced by blood-contacting devices. FXIIa also activates the kallikrein-kinin and

complement systems that generate the inflammation at the medical device site. Because FXIIa is dispensable for hemostasis, FXIIa inhibitors have been proposed as a safe alternative to current therapies.[2,5–7] Several animal studies and a monoclonal antibody in phase II clinical trials support this indication.[8–10] Beside its role in artificial surface-induced thrombosis, the pathophysiological role of FXIIa has been highlighted in diverse inflammatory disorders.[8,11–13] Garadacimab, an anti-FXIIa monoclonal antibody, is in phase III clinical trial for the prophylactic treatment of hereditary angioedema attacks.[14] FXIIa inhibition is also a promising therapeutic strategy in Alzheimer's disease since the discovery that beta-amyloid activates the contact system in a FXII-dependent manner. FXIIa was also proposed as a potential target in multiple sclerosis.[8]

FXIIa inhibitors under development are mainly peptides and proteins, including monoclonal antibodies, and, to a lesser extent, small-molecular weight inhibitors.[7,8] N-acylated azoles and peptidomimetics were recently described as potent and selective FXIIa inhibitors.[7,15–17] D. Kalinin's group[15–17] intensively produced analogs of a virtual HTS hit reported in the literature[18]. Their best acylated *1H*-1,2,4-triazol-5-amines selectively inhibit FXIIa through the formation of an acyl-enzyme complex and were active in the nanomolar range.[15–17] Beside these, our laboratory developed FXIIa inhibitors based on the coumarin scaffold.[19–21] The best compound of the series, 4-carbamimidamidophenyl 6-(chloromethyl)-2-oxo-*2H*-chromene-3-carboxylate (RF1), is a micromolar FXIIa inhibitor and its activity as a contact inhibitor was demonstrated in clotting time assays and whole blood[21], encouraging further modulations. In traditional medicinal chemistry, the hit-to-lead phase usually requires extensive chemical synthesis to obtain an appropriate lead compound, as illustrated by D. Kalinin's work[15–17] Alternatively, growing evidence highlight a synergistic effect when fragment-based drug discovery (FBDD) is used in tandem with another drug discovery approach.[22] Indeed, the FBDD strategy does not require extensive synthesis efforts and is a well-implemented approach to discover fragments that can be employed to construct lead compounds. Since fragments have a small size (molecular weight of less than 300 Da) and a low complexity, they are more susceptible to interact efficiently with the target. Consequently, the protein chemical space can be explored with a small library of less than thousands of compounds.[23,24]

In order to facilitate the chemical exploration of FXIIa active site and reduce the synthesis efforts, we thus applied a FBDD strategy. This article describes the optimization of our previous micromolar hit, RF1, into nanomolar inhibitors using a fragment approach.

▪ *Results and discussion*

Identification of hit fragments

FXIIa is a trypsin-like serine protease of the S1 family. This class of proteases is characterized by a deep, well-defined S1 pocket with Asp189 (chymotrypsin numbering scheme) at its base. The S1 site of these proteases recognizes an extended Arg residue through hydrogen-bonded salt-bridges with Asp189 and hydrophobic interactions with its walls. The S1 pocket is known to drive the major part of the association energy and most inhibitors of trypsin-like serine proteases include a S1-binding fragment to achieve high potency.[8,25] Regarding our scaffold, we hypothesized that the phenylguanidine moiety of RF1 is the S1-binding element (Figure 1). We determined the IC_{50} of the phenylguanidine fragment at 16.9 [15.5 – 18.4] mM (ligand efficiency (LE) of 0.32). We also evaluated 25 coumarins without the side chain at position 3. All of them were inactive, corroborating that this chain is crucial for the activity in our series. Our objective was thus to optimize the side chain interacting in S1. To spare chemical efforts, we decided first to explore the S1 pocket using a FBDD strategy and then to merge the best S1-binding fragments with the coumarin scaffold.

Herein, we report the approach that led to a nanomolar inhibitor of FXIIa with a 100-fold improvement compared to our initial hit.

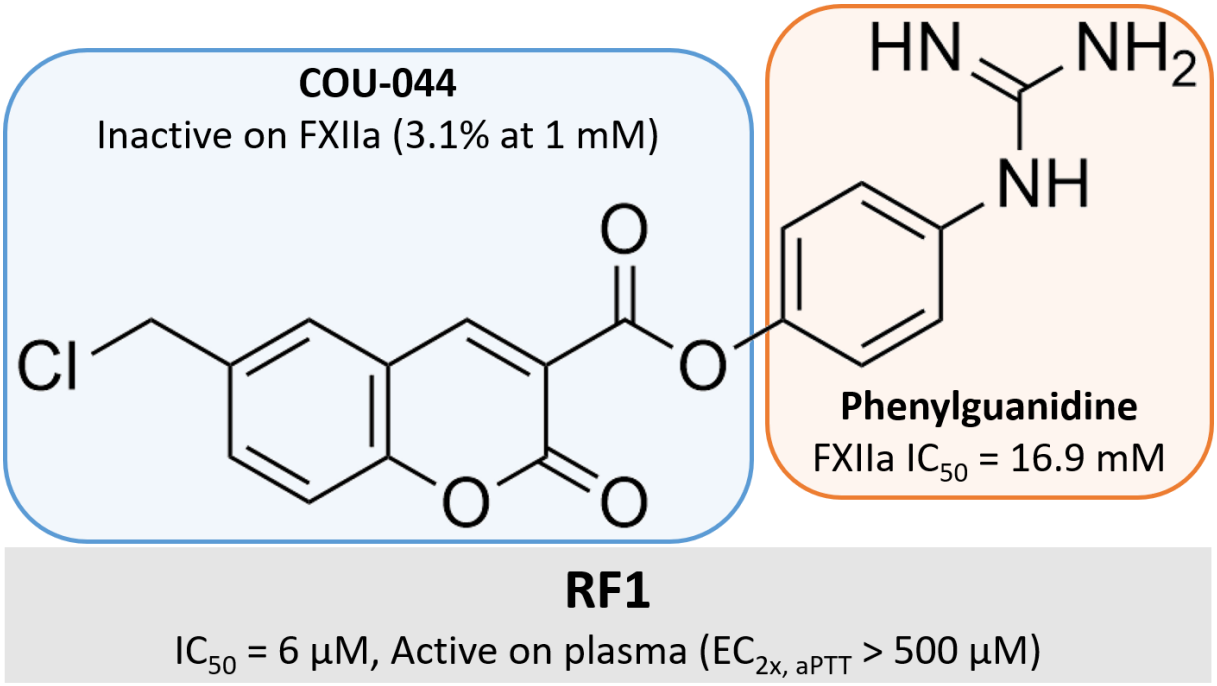

Figure 1. Structure of RF1, the initial hit of our series. $EC_{2x,\ aPTT}$: concentration required to prolong aPTT twice, IC_{50}: half maximal inhibitory concentration.

Biochemical assay optimization. Biochemical assays remain the most frequently used method for fragment-hit identification.[26] While an enzyme chromogenic assay was already developed for FXIIa in our laboratory[20,21], we observed an aberrant Hill slope when measuring the inhibitory potency (IC_{50}) of *p*-aminobenzamidine (PABZM), a weak affinity fragment. This result was attributed to an insufficient buffering capacity that was problematic, especially when mM range inhibitor concentrations are required. The buffer was further optimized to improve its buffering capacity by maintaining ionic strength and pH close to physiological conditions. The temperature was set to 37°C to maximize the enzyme activity. Assay linearity and DMSO tolerance were assessed with these new conditions. The assay was then validated according to the requirements described by the National Center for Advancing Translational Sciences.[27] In an orthogonal assay, we discovered that our screening assay was sensitive to low-level metallic impurities such as zinc and copper.[28] Consequently, all the hits from the biochemical assay were confirmed by performing the assay in the presence of 1 mM EDTA.

Library elaboration. In FBDD, the elaboration of the screening library is an important step to ensure the success. The selection of the fragments was based on three pillars. The first one is a knowledge-based approach in which we selected chemical motifs (amidine, guanidine, aminomethyl, amides, chloroaryl) known to interact with the S1 pocket on related serine proteases. The second pillar is a computer-based approach. We first extracted and virtually fragmented ligands present in complex with thrombin, factor Xa (FXa), and urokinase-type plasminogen activator. Then, we used the fragment subset of the MolPort Database[29] which contains over 239 000 fragments. A docking was done on the virtual library and the fragments with the higher glide efficient score and higher docking score were manually inspected to select the ones to incorporate. Finally, to increase the chemical diversity, we also decided to select fragments from our in-house compound library. As recommended for fragment elaboration[30], we limited the increase in size to 6 heavy atoms compared to

phenylguanidine moiety (heavy atom count ≤ 16), our starting fragment hit. At the end of the process, we selected 187 fragments and tested them with our biochemical assay.

Fragment screening. Table 1 summarizes the composition of the library in terms of functional motifs as well as the percentage of hits obtained. Most active compounds possess a basic functional group directly attached to an aromatic ring. The guanidine series was less potent than the amidine one. In the benzamidine series, different substitution patterns on benzene attached to an amidine were examined (see Supplemental Information – Table S1). Regarding the aromatic ring attached to the amidine, it appears that fused bicyclic aromatic ring such as naphthalene and quinoline were the most potent.

Table 1. Summary of the fragment screening. Nb.: number.

Functional motifs	Nb. of tested fragments	Nb. of fragments (%) with inhibition >30% at 1 mM	Nb. of fragments (%) with inhibition >60% at 1 mM
Amidine	30	11 (36%)	4 (13%)
Guanidine	7	0 (0%)	0 (0%)
Aminomethyl group	18	1 (5%)	0 (0%)
Aminopyridine and analogs	19	2 (10%)	1 (5%)
Amide	20	0 (0%)	0 (0%)
Halogenophenyl	26	0 (0%)	0 (0%)
Others	67	1 (1%)	0 (0%)
Total	**187**	**15 (8%)**	**5 (3%)**

Most of the compounds belonging to the other families were found to be inactive. Surprisingly, 1-aminoisoquinoline (Fragment **5**) was among the most potent (Figures 2 and 3). 1-Aminoisoquinoline was initially reported as a benzamidine (BZM) isostere with reduced basicity in the design of thrombin and FXa inhibitor.[31,32] In contrast with the previous reports[31,32], 1-aminoisoquinoline (LE = 0.52) was more efficient on FXIIa than benzamidine (LE = 0.45) (Figures 2 and 3). We also discovered a weakly active fragment, a benzothiazolidine (Fragment **6**, LE = 0.36), that was not previously described as a S1 binder (Figure 2). This fragment was highlighted by our virtual approach and confirmed during the screening. We also verified experimentally by Yonetani–Theorell analysis that this fragment is a S1 binder (see Supplemental Information – Figure S1).

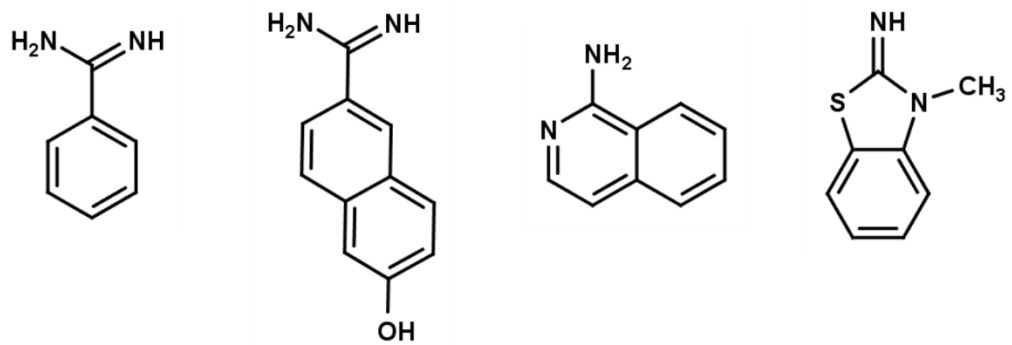

	Benzamidine	Fragment 2	Fragment 5	Fragment 6
Inhibition at 1 mM	34.4 %	69.6 %	70.6 %	31.5 %
IC_{50} (µM) ***[CI]*** **LE**	2377 *[2197 – 2557]* 0.45	386.7 *[365.3 – 408.1]* 0.37	399.9 *[374.3 – 425.6]* 0.52	2757 *[2547 – 2968]* 0.36

Figure 2. Structure of the fragment hits compared to benzamidine. CI: confidence interval at 95%, IC_{50}: half maximal inhibitory concentration, LE: ligand efficiency.

To further guide the selection of the fragments to be merged, we evaluated the selectivity of several fragments over several plasmatic trypsin-like serine proteases (Figure 3). We also tested bovine chymotrypsin as non-member of the trypsin-like serine protease group. To directly compare the IC_{50} of the fragments, the assays of others proteases were developed to maintain the same $[S]/K_m$ ratio (ratio of the substrate concentration to the Michaelis-Menten constant) as in the FXIIa assay. The assays' parameters, the determined K_m, and calculated K_i of BZM are available in the Supplemental Information (Tables S2 and S3). Phenylguanidine showed activity on FXIa, plasmin, and, to a lesser extent, kallikrein. This finding is consistent with the fact that RF1 was potent on kallikrein and FXIa in addition to FXIIa.[21] All amidines were active on all the trypsin-like serine proteases. However, large differences were observed in their potency. BZM was ≥ 5 times more potent on kallikrein, FXa, and plasmin than FXIIa. The two most potent fragments on FXIIa were 6-hydroxy-2-naphthimidamide (Fragment **2**) and 1-aminoisoquinoline (Fragment **5**). Fragment **2** was potent on all the trypsin-like serine proteases with a preference on kallikrein and plasmin. Fragment **5** was the most selective fragment for FXIIa (Figure 2 and 3).

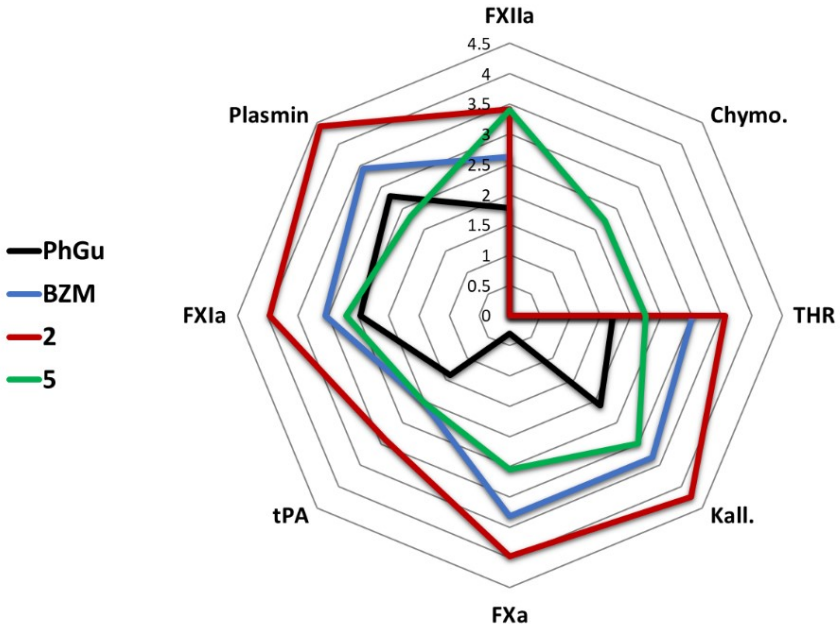

Figure 3. Selectivity profile of phenylguanidine (PhGu), benzamidine (BZM), fragment 2 (6-hydroxy-2-naphthimidamide), and fragment 5 (1-aminoisoquinoline) on plasmatic serine proteases and chymotrypsin. The values obtained are described in Table S4 (see Supplemental Information). Chymo: chymotrypsin, FXa: factor Xa, FXIa: factor XIa, FXIIa: factor XIIa, Kall.: kallikrein, THR: thrombin, tPA: tissue plasminogen activator.

Chemistry

Based on our fragment study, we selected Fragment **2** and Fragment **5** to be merged with our coumarin scaffold. Coumarins **12-22** and thiocoumarins **29-31** were obtained using the strategy depicted in Scheme 1and 2.[33–36] To synthesize 3-carboxycoumarins **9a-e**, salicylaldehyde derivatives **7** or 2,4,5-trimethoxybenzaldehyde **10g** were used according to their commercial availability. When starting with **7**, 3-carboxyethylestercoumarins **8a-g** were achieved by Knoevenagel condensation with diethyl malonate and then hydrolyzed to obtain **9a-g**. **9h** was obtained by protecting the alcohol of **9b** with a *tert*-butyldiphenylsilyl (TBDPS) group. When starting with **10g**, Meldrum's acid was used and the reaction yielded arylidene derivatives **11g** of Meldrum's acid through a Knoevenagel condensation. The cyclization of **11g** was realized by polyphosphoric acid dehydration. After dehydration, a mixture of 3-carboxycoumarin **9g** and 3-carboxymethylestercoumarins was obtained and was completely transformed into **9g** by hydrolysis.

Publisher version: https://doi.org/10.1016/j.ejmech.2023.115636

To synthesize 3-carboxythiocoumarins **28a-b** (scheme 2), 2-nitrobenzaldehyde derivatives **23** were converted into 2-(*tert*-butylsulfanyl)benzaldehyde derivatives **24** using *tert*-butylthiol through a nucleophilic aromatic substitution reaction. This reaction was initially performed in the presence of potassium carbonate (conditions of Meth-Cohn and Tarnowski[37]). However, when starting with 6-nitroveratraldehyde **23b**, the reaction required seven days to reach completion. Changing potassium carbonate by cesium carbonate reduced the reaction time for completion to 5 hours. A Knoevenagel condensation of **24** with ethyl 2-cyanoacetate or Meldrum's acid gave, respectively, **25** and **27**, which were further dehydrated and hydrolyzed to obtain **28**. 3-Carboxy(thio)coumarins **9** and **28** (scheme 1 and 2) were esterified via the formation of an acid chloride using thionyl chloride. The synthesis of **17** was performed by esterification of **9h** using 1-ethyl-3-(3-dimethylaminopropyl)carbodiimide (EDC) followed by TBDPS deprotection. Indeed, the TBDPS protective group of the benzoylalcohol was highly sensitive to acid. The deprotection occurred during the acid chloride formation even at stoichiometric amount of thionyl chloride in the presence of a neutralizing base.

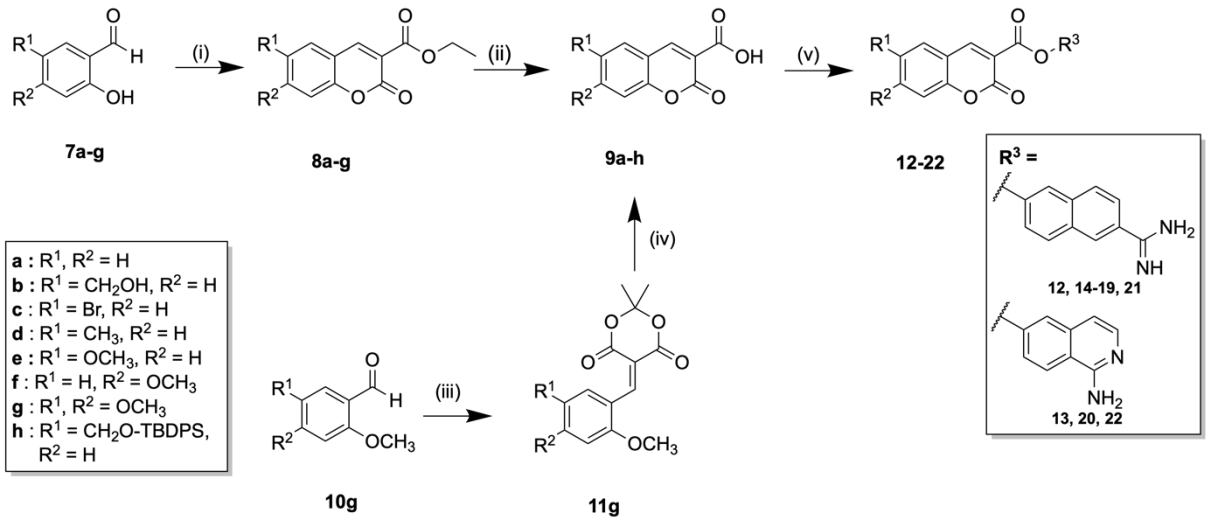

Scheme 1. Synthesis of the coumarin acid ester derivatives of Fragment 2 and Fragment 5. Reagents and conditions: (i) diethylmalonate, piperidine, AcOH, EtOH, reflux, 17 h; (ii) 1.10% NaOH, MW 140 °C, 11 min, 2.6 M HCl; (iii) Meldrum's acid, MeOH, rt, 1h; (iv) polyphosphoric acid, 100 °C, 3h; (v) Method A: 1. SOCl2, reflux, 3 h, 2. R3OH, pyridine, dioxane, DMF, 0 °C → rt, overnight, Method B: R3OH, EDC, DMAP, CH2Cl2, DMF, 0 °C → rt, overnight.

Publisher version: https://doi.org/10.1016/j.ejmech.2023.115636

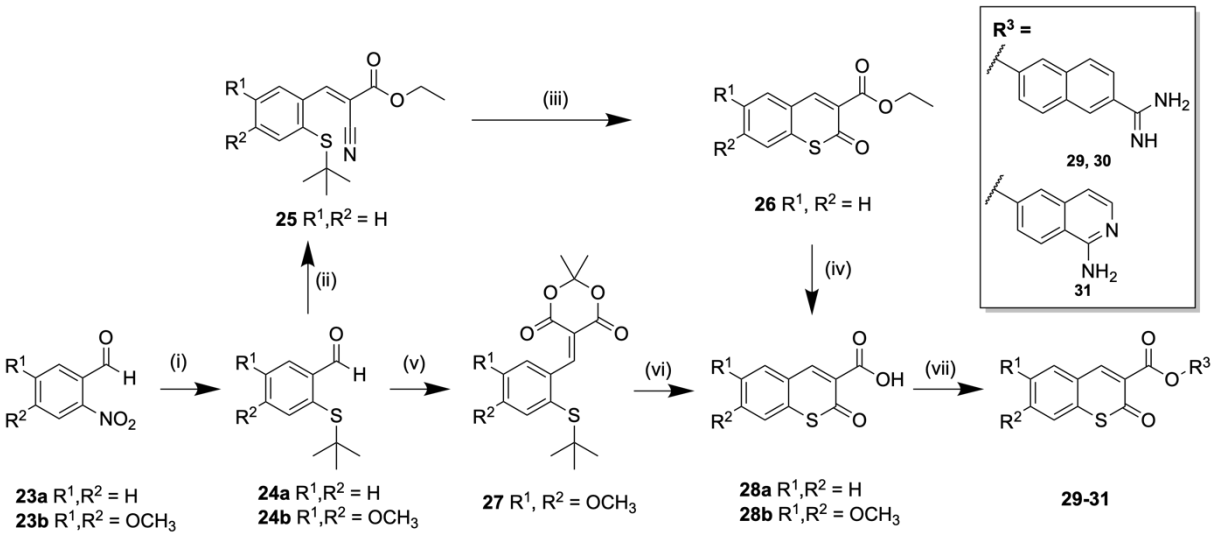

Scheme 2. Synthesis of the thiocoumarin acid ester derivatives of Fragment 2 and Fragment 5. Reagents and conditions: (i) Method A: tert-butylthiol, K2CO3, DMF, 100 °C, 30 h, Method B: tert-butylthiol, Ce2CO3, DMF, 80 °C, 5 h; (ii) ethyl 2-cyanoacetate, sodium ethanolate, EtOH, rt, 1.5 h; (iii) polyphosphoric acid, 100 °C, 40 min; (iv) 1.10% NaOH, MW 140 °C, 11 min, 2.6 M HCl; (v) Meldrum's acid, MeOH, rt, 24 h; (vi) polyphosphoric acid, 100 °C, 3h; (vii) 1. SOCl2, reflux, 3 h, 2. R3OH, pyridine, dioxane, DMF, 0 °C → rt, overnight.

The synthesis of 1-aminoisoquinolin-6-ol **36**, the required building block for the incorporation of Fragment **5** in our series, was achieved using the strategy depicted in Scheme 3. 6-Methoxyisoquinoline 2-oxide **33** was obtained by oxidation of 6-methoxyisoquinoline **32** using 3-chloroperoxybenzoic acid. We performed the amination of **33** using the conditions developed by Yin et al.[38], yielding 6-methoxyisoquinolin-1-amine **35** as a crude product. 1-Aminoisoquinolin-6-ol **36** was obtained by demethylation of crude product **35** using pyridinium chloride.

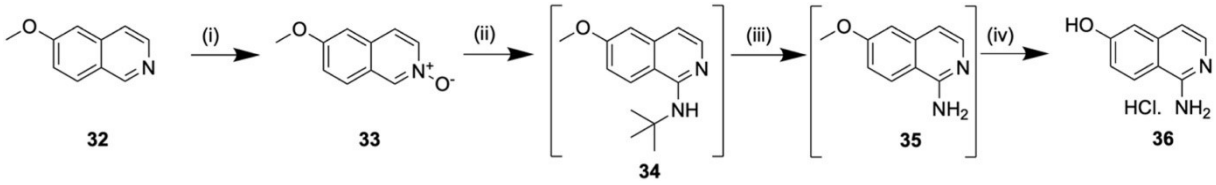

Scheme 2. Synthesis of 1-aminoisoquinolin-6-ol. Reagents and conditions: (i) mCPBA, CH_2Cl_2, rt, 3 h; (ii) *tert*-butylamine, Ts_2O, $CHCl_3$, 0°C, 1 h; (iii) 2M HCl (reduced pressure), 60°C, 30 min; (iv) pyridinium chloride, MW 200°C, 2.5h.

The synthetic pathway yielding *N*-(1-aminoisoquinolin-6-yl)-7-methoxy-2-oxo-*2H*-chromene-3-sulfonamide (**42**), the sulfonamide analog of **20**, is depicted in Scheme 4. From ethyl 2-chloroacetate (**37**), ethyl 2-(chlorosulfonyl)acetate (**39**) was obtained after reaction with Na_2SO_3 followed by chlorination according to a literature protocol.[39] 7-Methoxy-2-oxo-*2H*-chromene-3-sulfonamide (**41**) was synthesized from **39** as reported in the literature.[40] A Buchwald-Hartwig cross-coupling (conditions derived from Hickey et al.[41]) between **41** and the Boc-protected 6-bromoisoquinolin-1-amine followed by a Boc deprotection gave **42**.

Publisher version: https://doi.org/10.1016/j.ejmech.2023.115636

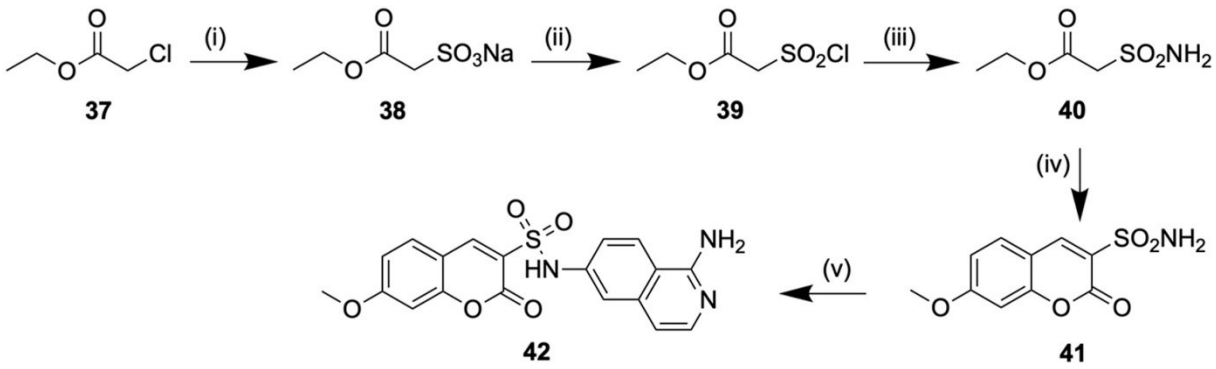

Scheme 3. Synthesis of *N*-(1-aminoisoquinolin-6-yl)-7-methoxy-2-oxo-*2H*-chromene-3-sulfonamide. Reagents and conditions: (i) Na_2SO_3, EtOH, H_2O, reflux, 18 h; (ii) $(COCl)_2$, DMF, CH_2Cl_2, rt, 16 h; (iii) 1. $HN(TMS)_2$, CH_2Cl_2, 0°C → rt, 1 h, 2. EtOH, rt, 45 min; (iv) 4-methoxysalicylaldehyde, piperidine, MW 130°C, 1 h; (v) 1. *tert*-butyl (6-bromoisoquinolin-1-yl)(*tert*-butoxycarbonyl)carbamate, *t*BuBrettPhos Pd G3, K_3PO_4, dry toluene, 100°C, 72 h, 2. 2M HCl in diethyl ether, MeOH, rt, 48h.

Biological evaluation

Enzymatic evaluation. The IC_{50} of the newly synthesized compounds was determined on FXIIa (Table 2). The replacement of the phenylguanidine moiety of RF1 by a naphthimidamide (**14**) results in a 7.5-fold increase in potency, confirming the validity of our FBDD strategy. To prevent unwanted off-target alkylation, we investigated the replacement of the chloromethyl group with various modulations on the coumarin ring. In contrary to what was observed with other proteases[33], the removal of the chloromethyl group did not totally suppress the inhibitory potency. Indeed, while a loss of activity was observed, coumarins without substituent (**12**, **13**) or with a methyl on the 6-position (**16**), had still a potency in the low µM ranges such as RF1. In the naphthimidamide series, we observed that the introduction of a hydroxymethyl (**17**), or a bromo (**15**) on the 6-position slightly increased the activity (between 1.3 and 2-fold increase). A moderate increase (between 2 and 5-fold increase) was observed with the chloromethyl group (**14**) and the methoxy group (**18**) in the same position. The best results (> 5-fold increase in activity) was obtained when a methoxy group is present on the 7-position (**19**, **21**). The most potent inhibitors were the one combining a methoxy group on both 6- and 7-position (**21**) with a IC_{50} value of about 60 nM.

The replacement of the naphthimidamide moiety by the isoquinoline one induced a slight (< 2-fold) decrease in potency (**13**, **20**, **22**, **31** vs **12**, **19**, **21**, **30**). Changing the coumarin ring by a thiocoumarin one did not improve the activity. As observed in the coumarin series, the introduction of 6,7-dimethoxy on the thiocoumarin ring (**30**, **31**) had a strong effect, but the potencies did not reach the ones obtained with **21** and **22**.

Publisher version: https://doi.org/10.1016/j.ejmech.2023.115636

Table 2. *In Vitro* FXIIa potency of Esters Derivatives. K_i^{app}: apparent inhibitory constant, IC_{50}: half maximal inhibitory concentration, Id.: identifier.

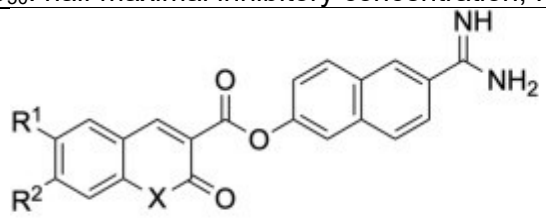

12, 14-19, 21, 29, 30

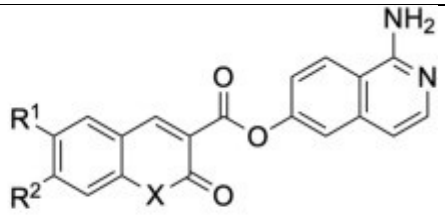

13, 20, 22, 31

Id.	R^1	R^2	Y	K_i^{app} FXIIa (nM)[a] (n=1)
12	H	H	O	4980 *[4180 – 5770]*
13	H	H	O	6600 *[4710 - 8480]*
14	CH_2Cl	H	O	802 *[754 – 850]*
15	Br	H	O	3610 *[3070 – 4160]*
16	CH_3	H	O	5190 *[4450 – 5930]*
17	CH_2OH	H	O	3950 *[3600 – 4300]*
18	OCH_3	H	O	1480 *[1330 – 1630]*
19	H	OCH_3	O	147 *[138 – 157]*
20	H	OCH_3	O	248 *[224 – 272]*
21	OCH_3	OCH_3	O	62.2 *[51.5 – 75.2]*
22	OCH_3	OCH_3	O	97.8 *[76.3 – 126]*
29	H	H	S	2230 *[1950 – 2520]*
30	6,7-O-CH_3	OCH_3	S	506 *[464 – 547]*
31	6,7-O-CH_3	OCH_3	S	529 *[470 – 588]*

[a] K_i^{app} is equal to the IC_{50} if the IC_{50} is above 10-fold the FXIIa concentration (> 131 nM).[42] If the IC_{50} is below 10-fold the FXIIa concentration, the data were treated using the Morrison equation to obtain the K_i^{app} (see Experimental Section). The confidence interval at 95% is mentioned in brackets.

Selectivity profile. The selectivity profile of the two most potent compounds (**21**, **22**) was investigated (Table 3). By comparison with the potency on FXIIa, we can classify the selectivity as inexistent (< 1.3-fold decrease), slight (between 1.3 and 2-fold decrease), moderate (between 2 and 10-fold decrease), strong (between 10 and 100-fold decrease), and very strong (> 100-fold decrease). The selectivity of compound **21** is slight towards plasmin (1.7-fold), strong towards thrombin and kallikrein (16- and 40-fold, respectively), and very strong towards the other serine proteases (chymotrypsin, FXa, tPA, and FXIa). Compound **22** exhibited a moderate selectivity towards thrombin (9-fold), a strong selectivity towards plasmin (22-fold), and a very strong selectivity towards the other serine proteases (chymotrypsin, kallikrein, FXa, tPA, and FXIa). Overall, **22** was more selective for FXIIa than **21**, which was expected since Fragment **5** was found more selective than Fragment **2**.

Table 3. Selectivity profile of the two most potent compounds (25, 26). Chymo.: chymotrypsin, FXa: factor Xa, FXIa: factor XIa, FXIIa: factor XIIa, K_i^{app}: apparent inhibitory constant, IC_{50}: half maximal inhibitory concentration, Id.: identifier, Kall.: kallikrein, THR: thrombin, tPA: tissue plasminogen activator.

	K_i^{app} (nM)[a] (n=1)	
Id.	**21**	**22**
FXIIa	62.2 *[51.5 – 75.2]*	97.8 *[76.3 – 126]*
Chymo.	>50000	>50000
THR	1000 *[890 – 1120]*	895 *[797 – 992]*
Kall.	2480 *[1850 – 3100]*	>50000
FXa	13200 *[10200 – 16200]*	>50000
tPA	>50000	>50000
FXIa	8640 *[5110 – 12200]*	>50000
Plasmin	106 *[84.4 – 133]*	2140 *[1740 – 2530]*

[a] K_i^{app} is equal to the IC_{50} if the IC_{50} is above 10-fold the enzyme concentration.[42] If the IC_{50} is below 10-fold the enzyme concentration, the data were treated using the Morrison equation to obtain the K_i^{app} (see Experimental Section). The confidence interval at 95% is mentioned in brackets.

Mechanism of inhibition. The 6-chloromethyl-scaffold has been designed as a mechanism-based inhibitor of serine proteases.[33,35,36,43,44] The proposed mechanism involves a nucleophilic attack by the serine on the lactone ring and the formation of an acyl-enzyme with *p*-hydroxybenzyl halide that could alkylate a nucleophilic residue in the active site. However, the behavior depends on the targeted enzyme. For chymotrypsin and thrombin, we observed the formation of an irreversible complex with a loss of the chlorine atom.[33,43] With human leucocyte elastase, we obtained a transient inhibition with the formation of a slowly-reversible enzyme inhibitor complex. With this enzyme, the chlorine atom from the 6-chloromethyl group could be replaced by a non-leaving group.[35]

A similar behavior was observed with FXIIa indicating that the alkylation step did not occur. Indeed, RF1 was found slowly reversible in jump-dilution experiment (see Supplemental Information – Figure S2). This suggests a reversible covalent inhibition with the formation of an acyl-enzyme. We performed intact mass protein analysis of FXIIa in the presence and absence of the two most potent inhibitors (**21**, **22**). In our experiment, we obtained a mass of 29497.4 Da for FXIIa, which is close to the mass reported in the literature.[15] In the presence of the inhibitors **21** and **22**, we obtained a mass shift for the enzyme-inhibitor complex of 232.0 Da (see Supplemental Information – Figure S3). These values agree with a mechanism that operates through acylation on the exocyclic ester (Figure 4).

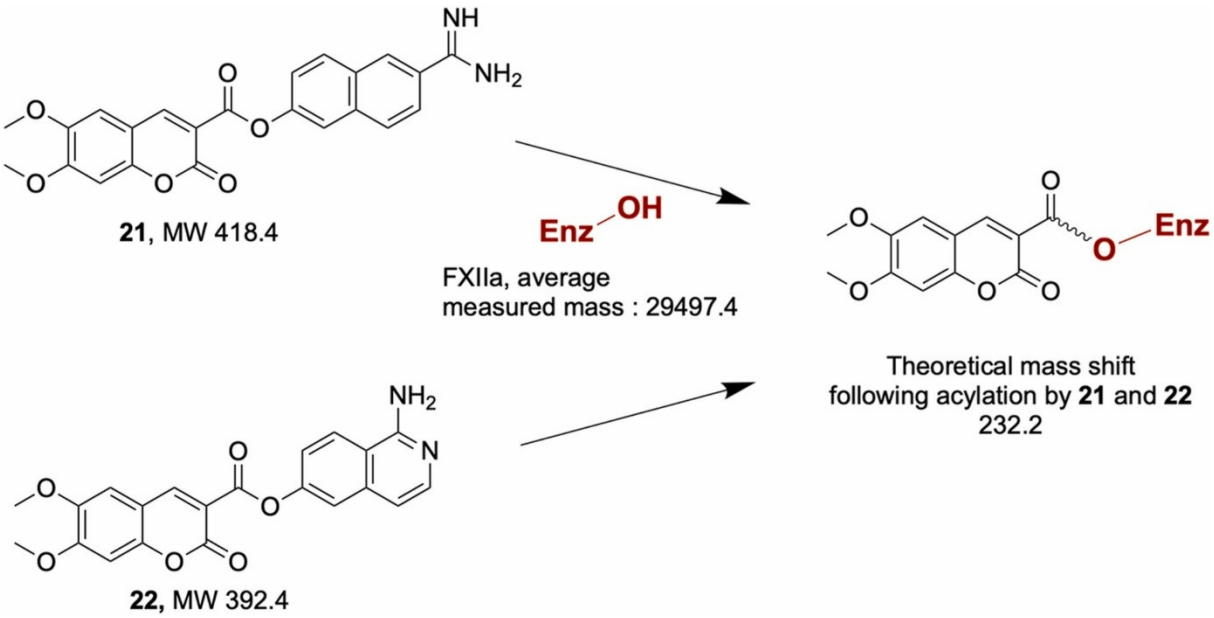

Figure 4. Theoretical masses for the studied compounds and the mass-shift of the related acylated enzyme. Enz: enzyme.

Biological activity. The routine laboratory tests for exploring the intrinsic and extrinsic coagulation pathways in plasma are the activated partial thromboplastin time (aPTT) and the prothrombin time (PT), respectively. A selective FXIIa inhibitor is expected to prolong the aPTT without affecting the PT.[21] We included rivaroxaban, a selective FXa inhibitor, as a positive control to verify if the collected pooled plasma behaved normally during aPTT and PT tests. In accordance with literature[15–17,45], rivaroxaban prolonged both aPTT and PT with a stronger effect on PT (Figure 5 and Table S5). Regarding the coumarin compounds, **21** strongly prolonged the aPTT while the PT was only slightly modified (Figure 5 and Table S5). Compound **22** also prolonged the aPTT but in a significantly lesser extent. The PT time with **22** did not increase. If we compare these results with those obtained with RF1 in the previous study[21], **21** is far more potent in plasma than RF1 which increases the aPTT only by a factor 1.7 at 500 µM. The concentration required to 2-fold increase the aPTT-clotting time ($EC_{2x,aPTT}$) was determined at 26.1 [19.5 – 34.2] µM for **21** (see Supplemental Information – Figure S4).

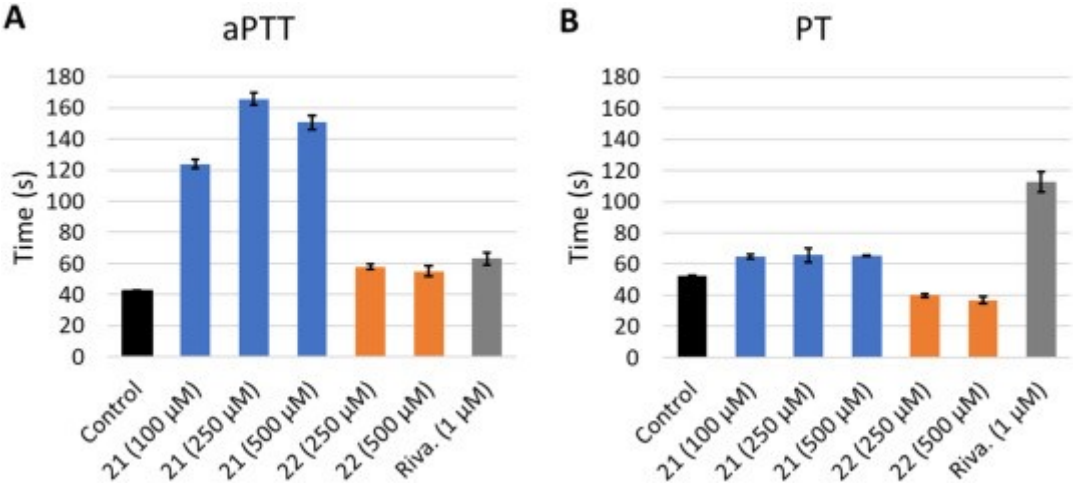

Figure 5. Effect of compounds 25, 26, and controls on aPTT and PT. The tested concentration is mentioned in brackets. The error bars correspond to the standard deviation (n=3). aPTT: activated partial thromboplastin time, PT: prothrombin time, Riva.: rivaroxaban.

Aqueous and plasmatic stabilities. Aqueous and plasmatic stabilities are important parameters to evaluate when developing new drugs. This is particularly true when the structures possess a hydrolytically labile function such as an ester.[46] To evaluate the stability of the two most potent compounds of our series (**21**, **22**), we determined their half-life ($t_{1/2}$) in phosphate-buffered saline (PBS) and platelet poor plasma using their fluorescence properties. Modulations of the coumarin ring with an electron-withdrawing element at 3-position (such as an ester) in combination with an electron-donating element at 7-position (such as a methoxy group) is known to produce high fluorescence quantum yields.[47] We observed that the excitation spectra of the esters and the corresponding acid was sufficiently different to allow the selective excitation of the esters (see Supplemental Information – Figure S5). So, the degradation of our compounds can be followed in real-time using their fluorescence properties, even in plasma (see Supplemental Information – Figure S6). In PBS, we determined the $t_{1/2}$ of **21** and **22** at 15.5 ± 0.3 h and 8.6 ± 0.1 h, respectively. In plasma, the $t_{1/2}$ of **21** and **22** were 1.9 ± 0.2 h and 0.7 ± 0.1 h, respectively (see Supplemental Information – Figure S7). Overall, **21** was less stable than **22**, which could explain the difference in potency during biological activity tests.

In an attempt to improve the stability, we modified the ester bond by a sulfonamide (Scheme 3). We did not investigate an amide linker since we previously observed that an amide link suppresses the inhibitory potency in our design on other serine proteases (chymotrypsin, human leukocyte elastase, thrombin, and FXa).[33,48] The amide function stabilizes an anti-conformation (carbonyl groups in opposite directions) through an intramolecular H bond.[48] The substitution of the ester bond (**20**) by the sulfonamide (**42**) induced a loss of potency (> 400-fold, FXIIa inhibition = 26.8% at 100 µM).

▪ *Conclusion*

In this article, we efficiently applied a FBDD strategy to improve the potency and selectivity of our coumarin series directed against FXIIa. Such strategy for optimizing hits is now widely used.[22] Fragments guide the optimization process without requiring the synthesis of complex chemical entities that can be difficult to produce. In our case, we were able to improve drastically the activity while synthesizing less than 15 compounds. Moreover, we found that even if the S1 pocket of trypsin-like serine proteases share a high homology, an optimization of the S1-binding element can exploit the small differences and bring selectivity. Overall, our best compounds **21**, **22** prove to be selective over various serine protases. Interestingly, compounds **21** is highly potent on the contact phase ($EC_{2x\ aPTT}$ 26.1 µM) with only moderate effect on the extrinsic coagulation pathway.

▪ *Experimental section*

Material and reagents

All chemical reagents and solvents were used as obtained by the chemical suppliers. ^{1}H NMR spectrum was recorded on a Jeol JNM EX 400 MHz or Jeol JNM-ECZR 500 MHz spectrometer with acetone-d_6 (residual internal acetone δ_H = 2.05 ppm), $CDCl_3$ (residual internal $CHCl_3$ δ_H = 7.26 ppm), or DMSO-d_6 (residual internal DMSO δ_H = 2.50 ppm) as solvent. All coupling constants are measured in Hertz (Hz), and the chemical shifts (δ_H) are quoted in parts per million (ppm) relative to tetramethylsilane (δ_0), which was used as the internal standard. Data are presented as follows: chemical shift, multiplicity (s = singlet, d = doublet, t = triplet, br = broad, m = multiplet), coupling constant (Hz), and integration. Automated flash chromatography was completed on a SP1 (Biotage, Uppsala, Sweden) or PuriFlash® 5.125 (Advion Interchim Scientific, Montluçon, France) system equipped with prepacked silica cartridges (FlashPure®, Buchi, Hendrik-Ido-Ambacht, Netherlands and PuriFlash®, Advion Interchim Scientific, Montluçon, France). For microwave-assisted synthesis, we used a Discover 2.0 apparatus (CEM, Matthews, NC, USA). Liquid Chromatography–mass spectra (LC–MS) were obtained using an Agilent 1100 LC/MSD trap

(Agilent Technologies, Santa Clara, CA, USA) with electrospray ionization (ESI) operating in positive ion mode, an autosampler, and a diode array detector. Purity evaluations were carried out with a C18 reverse-phase column (Zorbax SB-C18, 3.0 x 100 mm, particle size 3.5 µm, at 30 °C) using the following gradient of ultrapure water in acetonitrile (both modified with 0.1% formic acid, flow rate 0.5 mL/min): 0 min, 95% of water; 2 min, 95% of water; 12 min, 10% of water; 12.3 min, 10% of water; 13.3 min, 95% water; 16 min, 95% of water. All the final compounds are ≥95% pure by HPLC analysis. Confirmatory HPLC traces are included in the Supporting Information. Activity assays, biological evaluations, and stability experiments were performed on a multi-mode microplate reader SpectraMax iD3 (Molecular Devices, San Jose, CA, USA) operated by SoftMax Pro version 7.0.3 (Molecular Devices, San Jose, CA, USA). The instrument is equipped with plate shaking, injectors, and temperature control system (5°C above the ambient temperature to 66°C ± 1.0°C). Transparent 96-well flat-bottom polystyrene NBS microplates (Product No. 3641) were used for chromogenic assays and provided by Corning (New York, USA). Transparent 96-well flat-bottom polystyrene (used for biological assays) and black 96-well clear flat-bottom polystyrene microplates were sourced by Thermo Scientific™ (Waltham, MA, USA). Human plasma β-FXIIa, human Lys-plasmin, human factor XIa, human factor Xa, and human kallikrein were purchased from Innovative Research (Novi, MI, USA). Human thrombin was sourced from Roche (Mannheim, Germany). Bovine α-chymotrypsin, human tissue plasminogen activator human, and N-succinyl-Ala-Ala-Pro-Phe *p*-nitroanilide were obtained from Merck KGaA (Darmstadt, Germany). The substrates S-2302 and S-2366 was purchased from Werfen (Breda, Nederlands). The substrates pNAPEP-8503 and pNAPEP-9101 were purchased from Cryopep (Montpellier, France). Ultrapure water was produced by a Milli-Q equipment (Millipore, Bedford, MA, USA). Acrodisc® GHP syringe filters (0.2 µm) were obtained from Pall (Port Washington, NY, USA). Physico-chemical properties, such as aqueous solubility and pKa, were computed by MarvinSketch 19.27 (ChemAxon Ltd., Budapest, Hungary).

Chemistry

The syntheses of ethyl 2-oxo-*2H*-thiochromene-3-carboxylate (**26**)[37], 2,2-dimethyl-5-[(2,4,5-trimethoxyphenyl)methylidene]-1,3-dioxane-4,6-dione (**11g**)[49], 2-oxo-*2H*-chromene-3-carboxylic acid (**9a**)[35], 6-(hydroxymethyl)-2-oxo-2*H*-chromene-3-carboxylic acid (**9b**)[34], 6-bromo-2-oxo-2*H*-chromene-3-carboxylic acid (**9c**)[19], 6-methyl-2-oxo-2*H*-chromene-3-carboxylic acid (**9d**)[19], 6-methoxy-2-oxo-*2H*-chromene-3-carboxylic acid (**9e**)[50], 7-methoxy-2-oxo-2*H*-chromene-3-carboxylic acid (**9f**)[19], ethyl 2-(chlorosulfonyl)acetate (**39**)[39], ethyl 2-sulfamoylacetate (**40**)[40], 7-methoxy-2-oxo-*2H*-chromene-3-sulfonamide (**41**)[40], and *tert*-butyl (6-bromoisoquinolin-1-yl)(*tert*-butoxycarbonyl)carbamate[51] were previously described.

General procedure A for the hydrolysis of (thio)coumarin-3-carboxylate Esters

NaOH 10% (2 mL/mmol) was added to the appropriate coumarin-3-carboxylate ester and heated at 140°C (microwave, 11 min). The solution was neutralized with HCl 6M (10 mL/mmol). The precipitate was filtrated, washed with water (10 mL/mmol, 3 times), and dried to afford the corresponding coumarin-3-carboxylic acid.

General procedure B for the synthesis of coumarin-3-carboxylate acid esters of Fragment 2 (12, 14-16, 18, 19, 21, 29, and 30)

Thionyl chloride (7.5 mL/mmol) was poured into a flask containing the appropriate coumarin-3-carboxylic acid (1.875 equiv). The solution was stirred and refluxed for 3 h. After cooling, the mixture was evaporated under reduced pressure. The residue was suspended in anhydrous toluene (7.5 mL/mmol) and then evaporated under reduced pressure. This step was repeated three times. The resulting acyl chloride was suspended in anhydrous dioxane. The 6-amidino-2-naphthol methanesulfonate (1 equiv) and dry pyridine (1.1 equiv) were dissolved in anhydrous DMF (6.8 mL/mmol) and cooled on ice under an argon atmosphere. To this solution, the suspension of acyl chloride was added portion wise (1 mL fraction). The

mixture was stirred overnight under an argon atmosphere and allowed to return at room temperature.

General procedure C for the synthesis of (thio)coumarin-3-carboxylate acid esters of Fragment 5 (13, 20, 22, 31)

The procedure was similar to the general procedure B, except that 1 equivalent of the appropriate coumarin-3-carboxylic acid (instead of 1.875 equiv) and 1-aminoisoquinolin-6-ol hydrochloride **34** (instead of 6-amidino-2-naphthol methanesulfonate) were used.

General procedure D for the purification of (thio)coumarin-3-carboxylate acid esters of Fragment 2 by flash chromatography

The product was isolated using an automated flash chromatography equipped with a silica cartridge. The flow rate recommended for the column was used. The following gradient of isopropanol in acetonitrile (both modified with 0.1% formic acid) was applied: the elution started with an isopropanol/acetonitrile ratio of 30%/70% for 4 column volumes, then the ratio increased to 55%/45% over 3 column volumes and hold for 8 column volumes. The product detection was followed by UV absorption at 254, 280, 260, 232, and 200-400 nm. The collection was threshold-based using the UV signal at 200-400 nm. The collected fractions containing the product were combined.

General procedure E for the counter-ion exchange of (thio)coumarin-3-carboxylate acid esters

After evaporation, the appropriate coumarin-3-carboxylate esters was dissolved in methanol:acetonitrile (70:30). The solution was acidified by 5 mL methanolic HCl (3M). After evaporation of 80 % of the volume, the precipitate was collected, washed with acetone (5 mL, 3 times), and dried.

6,7-Dimethoxy-2-oxo-2H-chromene-3-carboxylic acid (9g)

11g (5.9 mmol, 1.9 g) was mixed with polyphosphoric acid (22 g) at 80°C during 20 min. Crushed ice (150 mL) was added. The precipitate was filtrated and washed with water (1 mL, 3 times). Due to the presence of methyl 6,7-dimethoxy-2-oxo-*2H*-chromene-3-carboxylate, a hydrolysis was performed on the crude product. The general procedure A afforded **9g** as a yellow powder (1.19 g, 81%). The structural features were in accordance with previously published data.[52]

2-Oxo-2H-thiochromene-3-carboxylic acid (28a)

26 (4.3 mmol, 1g) was dissolved into ethanol: HCl 3M (1:75, 100 mL) and refluxed for 3h. After cooling, the precipitate was filtrated, washed with water, and crystallized in acetonitrile to afford 2-oxo-*2H*-thiochromene-3-carboxylic acid as a white powder (555 mg, 63%). Spectral data were in accordance with previously published data.[53]

6,7-Dimethoxy-2-oxo-2H-thiochromene-3-carboxylic acid (28b)

tert-Butylthiol (13.3 mmol, 1.5 mL, 1.1 equiv.) was poured at room temperature into a flask containing a solution of 6-nitroveratraldehyde (11.8 mmol, 2.5 g) and cesium carbonate (14.4 mmol, 4.6 g, 1.2 equiv) dissolved in DMF (18 mL). The solution was stirred and heated at 80°C for 5h. The mixture was cooled at room temperature, H_2O (72 mL) was added, and the mixture was extracted with di-isopropylether:ethylacetate (9:1, 100 mL, 3 times). The organic layers were washed with aq. sat. NH_4Cl solution and brine, dried with $MgSO_4$, and the solvents were evaporated under reduced pressure. Meldrum's acid (14.4 mmol, 2.1 g) and methanol (10 mL) was added to the crude product containing mainly 2-(*tert*-butylsulfanyl)-4,5-dimethoxybenzaldehyde. The resulting solution was stirred at room temperature for 24h. Polyphosphoric acid (~45 g) was added and heated at 100°C for 3h. Crushed ice (200 mL)

was added. The precipitate was filtrated, washed with water (50 mL, 3 times), and dried. **28b** was isolated using the automated flash chromatography. The flowrate was fixed at 32 mL/min and a FlashPure EcoFlex Silica 24g column was used. The following gradient of ethyl acetate in acetonitrile was applied: the elution started with ethyl acetate for 10 column volumes, then the acetonitrile increased to 100% over 30 column volumes and hold for 8 column volumes. The product detection was followed by UV absorption at 254, 280, 260, 232, and 200-400 nm. The collection was threshold-based using the UV signal at 200-400 nm. The collected fractions containing **28b** were combined. After evaporation, the pure product was collected as a yellow powder (250 mg, 28%). ^{1}H NMR (400 MHz, DMSO-d_6): δ_H (ppm) 8.63 (s, 1H, HC=C), 7.72 (s, 1H, ArH), 7.35 (s, 1H, ArH), 3.91 (s, 3H, O-CH_3), 3.85 (s, 3H, O-CH_3). LC–MS (ESI) *m/z*: 267.1 (MS calcld for $C_{12}H_{11}O_5S$ $[M+H]^+$, 267.0), t_R = 9.9 min, purity > 95% (UV).

6-Carbamimidoylnaphthalen-2-yl 2-oxo-2H-chromene-3-carboxylate methanesulfonate (12)

Following the general procedure B, **9a** and 6-amidino-2-naphthol methanesulfonate (0.664 mmol, 187 mg) gave **12** as a crude mixture. The mixture was cooled. The precipitate was filtrated and washed four times with cooled DMF:dioxane (50:50, 500 µL). **12** was isolated from the precipitate using the automated flash chromatography (PuriFlash® 5.125) with the FlashPure EcoFlex Silica Solid Loader 20g column (general procedure D). The pure product was collected as an off-white solid (102 mg, 34%).^{1}H NMR (500 MHz, DMSO-d_6): δ_H (ppm) 9.56 (s, 2H, NH_2), 9.29 (s, 2H, NH_2), 9.20 (s, 1H, HC=C), 8.60 (d, J = 1.7 Hz, 1H, ArH), 8.19-8.25 (m, 2H, ArH), 8.02-8.05 (m, 2H, ArH), 7.88-7.91 (m, 1H, ArH), 7.83 (td, J = 7.7, 1.5 Hz, 1H, ArH), 7.66 (dd, J = 8.6, 2.3 Hz, 1H, ArH), 7.47-7.54 (m, 2H, ArH), 2.32 (s, 3H, H_3C-SO_3^-). LC–MS (ESI) *m/z*: 359.2 (MS calcld for $C_{21}H_{15}N_2O_4$ $[M+H]^+$, 359.1), t_R = 9.1 min, purity > 95% (UV).

1-Aminoisoquinolin-6-yl 2-oxo-2H-chromene-3-carboxylate hydrochloride (13)

Following the general procedure C, **9a** and **36** (0.375 mmol, 60 mg) gave **13** as a crude mixture. The dioxane was evaporated under reduced pressure. The precipitate was filtrated. **13** was isolated from the precipitate using the automated flash chromatography (PuriFlash) with the FlashPure EcoFlex Silica 12g column. The flow rate was fixed at 25 mL/min. The following gradient of isopropanol in acetonitrile (both modified with 0.1% formic acid) was applied: the elution started with an isopropanol/acetonitrile ratio of 40%/60% for 2 column volumes, then the ratio increased to 50%/50% over 6 column volumes and hold for 7 column volumes. The product detection was followed by UV absorption at 254, 280, 260, 232, and 200-400 nm. The collection was threshold-based using the UV signal at 200-400 nm. The collected fractions containing the product were combined. The pure product was collected as an off-white solid (15.5 mg, 11%). ^{1}H NMR (400 MHz, DMSO-d_6): δ_H (ppm) 9.20 (s, 1H, HC=C), 8.93 (brs, 2H, NH_2), 8.69 (d, J = 9.2 Hz, 1H, ArH), 8.03 (dd, J = 7.9, 1.5 Hz, 1H, ArH), 7.90 (d, J = 2.3 Hz, 1H, ArH), 7.81-7.86 (m, 1H, ArH), 7.70-7.77 (m, 2H, ArH), 7.47-7.54 (m, 2H, ArH), 7.23 (d, J = 6.9 Hz, 1H, ArH). LC–MS (ESI) *m/z*: 332.2 (MS calcld for $C_{19}H_{12}N_2O_4$ $[M+H]^+$, 332.1), t_R = 8.6 min, purity > 95% (UV).

6-Carbamimidoylnaphthalen-2-yl 6-(chloromethyl)-2-oxo-2H-chromene-3-carboxylate hydrochloride (14)

Following the general procedure B, **9b** and 6-amidino-2-naphthol methanesulfonate (0.664 mmol, 187 mg) gave **14** as a crude mixture. The dioxane was evaporated. Water adjusted at pH 2 with fuming HCl was added. The precipitate was filtrated and washed three times with acetone to give **14** as an orangish solid (54 mg, 20%). ^{1}H NMR (400 MHz, DMSO-d_6): δ_H (ppm) 9.57 (s, 2H, NH_2), 9.29 (s, 2H, NH_2), 9.18 (s, 1H, HC=C), 8.59 (s, 1H, ArH), 8.25-7.87 (m, 6H, ArH), 7.67-7.53 (m, 2H, ArH), 4.90 (s, 2H, Ar-CH_2-Cl). LC–MS (ESI) *m/z*: 407.2 (MS calcld for $C_{22}H_{16}ClN_2O_4$ $[M+H]^+$, 407.1), t_R = 9.8 min, purity > 95% (UV).

6-Carbamimidoylnaphthalen-2-yl 6-bromo-2-oxo-2H-chromene-3-carboxylate hydrochloride (15)

Following the general procedure B, **9c** and 6-amidino-2-naphthol methanesulfonate (0.664 mmol, 187 mg) gave **15** as a crude mixture. The precipitate was filtrated. **15** was isolated from the precipitate using the automated flash chromatography (PuriFlash® 5.125) with the FlashPure EcoFlex Silica 12g column (general procedure D). After evaporation, the counter-ion of the amidine was completely exchanged to hydrochloride following the general procedure E. The pure product was collected as an off-white solid (13.6 mg, off-white, 4%). ^{1}H NMR (400 MHz, DMSO-d_6): δ_H (ppm) 9.55 (s, 2H, NH_2), 9.26 (s, 2H, NH_2), 9.13 (s, 1H, HC=C), 8.59 (s, 1H, ArH), 8.30 (d, J = 2.3 Hz, 1H, ArH), 8.23 (t, J = 9.8 Hz, 2H, ArH), 7.96-8.02 (m, 2H, ArH), 7.90 (d, J = 8.5 Hz, 1H, ArH), 7.65 (dd, J = 8.9, 1.6 Hz, 1H, ArH), 7.51 (d, J = 8.9 Hz, 1H, ArH). LC–MS (ESI) *m/z*: 437.4 (MS calcld for $C_{21}H_{14}BrN_2O_4$ $[M+H]^+$, 437.0), t_R = 9.8 min, purity > 95% (UV).

6-Carbamimidoylnaphthalen-2-yl 6-methyl-2-oxo-2H-chromene-3-carboxylate hydrochloride (16)

Following the general procedure B, **9d** and 6-amidino-2-naphthol methanesulfonate (0.664 mmol, 187 mg) gave **16** as a crude mixture. The precipitate was filtrated. **16** was isolated from the precipitate using the automated flash chromatography (PuriFlash) with the FlashPure EcoFlex Silica 12g column (general procedure D). After evaporation, the counter-ion of the amidine was completely exchanged to hydrochloride following the general procedure E. The pure product was collected as a yellowish solid (73.8 mg, 27%). ^{1}H NMR (400 MHz, DMSO-d_6): δ_H (ppm) 9.53 (s, 2H, NH_2), 9.20 (s, 2H, NH_2), 9.11 (s, 1H, HC=C), 8.58 (s, 1H, ArH), 8.23 (dd, J = 11.7, 8.9 Hz, 2H, ArH), 8.02 (d, J = 2.1 Hz, 1H, ArH), 7.89 (dd, J = 8.6, 1.5 Hz, 1H, ArH), 7.81 (s, 1H, ArH), 7.66 (dd, J = 8.8, 1.7 Hz, 2H, ArH), 7.44 (d, J = 8.7 Hz, 1H, ArH), 2.42 (s, 3H, $-CH_3$). LC–MS (ESI) *m/z*: 373.2 (MS calcld for $C_{22}H_{17}N_2O_4$ $[M+H]^+$, 373.1), t_R = 9.4 min, purity > 95% (UV).

6-Carbamimidoylnaphthalen-2-yl 6-(hydroxymethyl)-2-oxo-2H-chromene-3-carboxylate hydrochloride (17)

Imidazole (10.3 mmol, 700 mg, 2.2 equiv) and **9b** (4.5 mmol, 1 g, 1 equiv) were dissolved in DMF (7 mL). *tert*-Butyl(chloro)diphenylsilane (4.9 mmol, 1.35 g, 1.1 equiv) was added to the stirred solution. Stirring was maintained for 4 h at rt. The solution was chilled and the precipitate was filtrated, washed with methanol (3 times, 10 mL), and dried. The crude product containing 6-{[(*tert*-butyldiphenylsilyl)oxy]methyl}-2-oxo-*2H*-chromene-3-carboxylic acid (**9h** LC-MS: 87%, 459.3, MS calcld for $C_{27}H_{27}O_5Si$ $[M+H]^+$: 459.2) was used without further purification.

The crude product **9h** (0.664 mmol, 350 mg, 1 equiv) and EDC hydrochloride (1.992 mmol, 381 mg, 3 equiv) were dissolved in dry CH_2Cl_2 (4.5 mL) and cooled to 0°C. A solution of 6-amidino-2-naphthol methanesulfonate (1.992 mmol, 562 mg, 3 equiv) and DMAP (0.100 mmol, 12 mg, 0.15 equiv) in dry DMF (4.5 mL) was added to the latter. The resulting solution was stirred overnight. Dichloromethane was evaporated under reduced pressure. DMF was acidified with 6M HCl (200 µL) and the solution was stirred for 30 min. 0.45 M HCl in water (20 mL) was added. The precipitate was harvested by filtration. **17** was isolated from the precipitate using the automated flash chromatography (PuriFlash® 5.125) with the FlashPure EcoFlex Silica 12g column. The flow rate was fixed at 25 mL/min. The following gradient of isopropanol in acetonitrile (both modified with 0.1% formic acid) was applied: the elution started with an isopropanol/acetonitrile ratio of 25%/85% for 3 column volumes, then the ratio increased to 40%/60% over 5 column volumes, hold for 8 column volumes, then the ratio increased to 60%/40% over 12 column volumes, and hold for 6 column volumes. The product detection was followed by UV absorption at 254, 280, 260, 232, and 200-400 nm. The collection was threshold-based using the UV signal at 200-400 nm. The collected fractions containing the product were combined. The pure product was collected as an off-white solid

(2.0 mg, 1%). ^{1}H NMR (400 MHz, DMSO-d_6): δ_H (ppm) 9.53 (s, 2H, NH_2), 9.20 (s, 2H, NH_2), 9.18 (s, 1H, HC=C), 8.58 (s, 1H, ArH), 8.23 (dd, J = 11.6, 9.0 Hz, 2H, ArH), 8.03 (s, 1H, ArH), 7.88-7.94 (m, 2H, ArH), 7.66-7.77 (m, 2H, ArH), 7.48-7.52 (m, 1H, ArH), 5.49 (t, J = 5.6 Hz, 1H, -OH), 4.60 (d, J = 5.7 Hz, 2H, -CH_2-O). LC–MS (ESI) *m/z*: 389.2 (MS calcld for $C_{22}H_{17}N_2O_4$ $[M+H]^+$, 389.1), t_R = 8.5 min, purity > 95% (UV).

6-Carbamimidoylnaphthalen-2-yl 6-methoxy-2-oxo-2H-chromene-3-carboxylate methanesulfonate (18)

Following the general procedure B, **9e** and 6-amidino-2-naphthol methanesulfonate (0.664 mmol, 187 mg) gave **18** as a crude mixture. The precipitate was discarded and diisopropylether was added to the filtrate. The resulting precipitate was filtrated and washed three times with diisopropylether to give **18** as a yellow solid (11.6 mg, 4%). ^{1}H NMR (400 MHz, DMSO-d_6): δ_H (ppm) 9.50 (s, 2H, NH_2), 9.13 (s, 2H, NH_2), 9.11 (s, 1H, HC=C), 8.57 (s, 1H, ArH), 8.23 (t, J = 10.3 Hz, 2H, ArH), 7.88-8.02 (m, 2H, ArH), 7.61-7.73 (m, 2H, ArH), 7.42-7.50 (m, 2H, ArH), 3.85 (s, 3H, O-CH_3), 2.32 (s, 3H, H_3C-SO_3^-). LC–MS (ESI) *m/z*: 389.2 (MS calcld for $C_{22}H_{17}N_2O_5$ $[M+H]^+$, 389.1), t_R = 9.4 min, purity > 95% (UV).

6-Carbamimidoylnaphthalen-2-yl 7-methoxy-2-oxo-2H-chromene-3-carboxylate hydrochloride (19)

Following the general procedure B, **9f** and 6-amidino-2-naphthol methanesulfonate (0.664 mmol, 187 mg) gave **19** as an impure mixture. The precipitate was filtrated, washed six times with cold dioxane:DMF (50:50, 500 µL), and dried to give **19** as an off-white solid (47 mg, 17%). ^{1}H NMR (400 MHz, DMSO-d_6): δ_H (ppm) 9.53 (s, 2H, NH_2), 9.20 (s, 2H, NH_2), 9.14 (s, 1H, HC=C), 8.57 (s, 1H, ArH), 8.21 (t, J = 10.2 Hz, 2H, ArH), 7.87-7.99 (m, 3H, ArH), 7.64 (d, J = 8.9 Hz, 1H, ArH), 7.07-7.13 (m, 2H, ArH), 3.93 (s, 3H, O-CH_3). LC–MS (ESI) *m/z*: 389.2 (MS calcld for $C_{22}H_{17}N_2O_5$ $[M+H]^+$, 389.1), t_R = 9.3 min, purity > 95% (UV).

1-Aminoisoquinolin-6-yl 7-methoxy-2-oxo-2H-chromene-3-carboxylate hydrochloride (20)

Following the general procedure C, **9f** and **36** (0.661 mmol, 130 mg) gave **20** as a crude mixture. The precipitate was eliminated by filtration. Acetone was added to the filtrate. The resulting precipitate was filtrated and washed three times with acetone to give **20** as a yellowish solid (24.2 mg, 9%). ^{1}H NMR (500 MHz, DMSO-d_6): δ_H (ppm) 9.14 (s, 1H, HC=C), 9.05 (brs, 2H, NH_2), 8.72 (d, J = 9.2 Hz,1H, ArH), 7.90-8.00 (m, 2H, ArH), 7.72-7.76 (m, 2H, ArH), 7.24 (d, J = 6.9 Hz, 1H, ArH), 7.15 (dd, J = 17.2, 2.3 Hz, 1H, ArH), 7.05-7.10 (m, 1H, ArH), 3.94 (s, 3H, O-CH_3). LC–MS (ESI) *m/z*: 363.2 (MS calcld for $C_{20}H_{15}N_2O_5$ $[M+H]^+$, 363.1), t_R = 9.3 min, purity > 95% (UV).

6-Carbamimidoylnaphthalen-2-yl 6,7-dimethoxy-2-oxo-2H-chromene-3-carboxylate hydrochloride (21)

Following the general procedure B, **9g** and 6-amidino-2-naphthol methanesulfonate (0.664 mmol, 187 mg) gave **21** as a crude mixture. The dioxane was evaporated under reduced pressure. The solution was acidified by 6M HCl (100 µL). The addition of 0.45M HCl in water (20 mL) generated a precipitate. **21** was isolated from the precipitate using the automated flash chromatography (PuriFlash) with the FlashPure EcoFlex Silica 24g column (general procedure D). After evaporation, the counter-ion of the amidine was completely exchanged to hydrochloride following the general procedure E. The pure product was collected as a yellow solid (18.5 mg, 6%). ^{1}H NMR (400 MHz, DMSO-d_6): δ_H (ppm) 9.55 (s, 2H, NH_2), 9.25 (s, 2H, NH_2), 9.10 (s, 1H, HC=C), 8.58 (s, 1H, ArH), 8.21 (dd, J = 11.4, 8.9 Hz, 2H, ArH), 8.00 (d, J = 2.1 Hz, 1H, ArH), 7.89 (dd, J = 8.6, 1.7 Hz, 1H, ArH), 7.64 (dd, J = 8.8, 2.2 Hz, 1H, ArH), 7.57 (s, 1H, ArH), 7.21 (s, 1H, ArH), 3.93 (s, 3H, O-CH_3), 3.84 (s, 3H, O-CH_3). LC–MS (ESI) *m/z*: 419.2 (MS calcld for $C_{23}H_{19}N_2O_6$ $[M+H]^+$, 419.1), t_R = 9.1 min, purity > 95% (UV).

1-Aminoisoquinolin-6-yl 6,7-dimethoxy-2-oxo-2H-chromene-3-carboxylate hydrochloride (22)

Following the general procedure C, **9g** and **36** (0.661 mmol, 130 mg) gave **22** as a crude mixture. The dioxane was evaporated under reduced pressure. The precipitate was filtrated. **22** was isolated from the precipitate using the automated flash chromatography (PuriFlash) with the FlashPure EcoFlex Silica 25g column. The flow rate was 21 mL/min. The following gradient of isopropanol in acetonitrile (both modified with 0.1% formic acid) was applied: the elution started with an isopropanol/acetonitrile ratio of 25%/75% for 6 column volumes, then the ratio increased to 40%/60% over 4 column volumes, then the ratio increased to 70%/30% over 2 column volume, and hold for 4 column volumes. The product detection was followed by UV absorption at 254, 280, 260, 232, and 200-400 nm. The collection was threshold-based using the UV signal at 200-400 nm. The collected fractions containing the product were combined. The pure product was collected as an orange solid (64.6 mg, 23%). ^{1}H NMR (500 MHz, DMSO-d_6): δ_H (ppm) 9.21 (brs, 2H, NH_2), 9.09 (s, 1H, HC=C), 8.72 (d, J = 9.2 Hz, 1H, ArH), 7.90 (d, J = 1.7 Hz, 1H, ArH), 7.72-7.76 (m, 2H, ArH), 7.56 (s, 1H, ArH), 7.24-7.28 (m, 1H, ArH), 7.20 (s, 1H, ArH), 3.96 (s, 3H, O-CH_3), 3.82 (s, 3H, O-CH_3). LC–MS (ESI) *m/z*: 393.2 (MS calcld for $C_{21}H_{17}N_2O_6$ $[M+H]^+$, 393.1), t_R = 8.9 min, purity > 95% (UV).

6-Carbamimidoylnaphthalen-2-yl 2-oxo-2H-thiochromene-3-carboxylate methanesulfonate (29)

Following the general procedure B, **28a** and 6-amidino-2-naphthol methanesulfonate (0.664 mmol, 187 mg) gave **29** as a crude mixture. The crude mixture was cooled. The precipitate was filtrated, washed with cooled DMF:dioxane (50:50, 750 µL, 8 times) and cyclohexane (750 µL, 8 times), and dried. **29** was isolated from the precipitate using the automated flash chromatography (Biotage) with the PuriFlash® 12g SI-HC 15 µm (spherical silica of 15 µm) column. The flow rate was fixed at 20 mL/min. The separation was performed in isocratic mode using methanol/acetonitrile 10:90 (both modified with 0.1% formic acid). The product detection was followed by UV absorption at 254 and 300 nm. All fractions were collected. The fractions containing **27** were combined. After evaporation, the pure product was collected as an orangish solid (40.6 mg, 13%). ^{1}H NMR (400 MHz, DMSO-d_6): δ_H (ppm) 9.48 (s, 2H, NH_2), 9.07 (s, 2H, NH_2), 9.06 (s, 1H, HC=C), 8.56 (s, 1H, ArH), 8.19-8.26 (m, 3H, ArH), 8.03 (d, J = 1.8 Hz, 1H, ArH), 7.88 (d, J = 8.5 Hz, 1H), 7.77-7.81 (m, 2H, ArH), 7.60-7.68 (m, 2H, ArH), 2.32 (s, 3H, H_3C-SO_3^-). LC–MS (ESI) *m/z*: 375.2 (MS calcd for $C_{21}H_{15}N_2O_3S$ $[M+H]^+$, 375.1), t_R = 9.8 min, purity > 95% (UV).

6-Carbamimidoylnaphthalen-2-yl 6,7-dimethoxy-2-oxo-2H-thiochromene-3-carboxylate hydrochloride (30)

Following the general procedure B, **28b** and 6-amidino-2-naphthol methanesulfonate (0.332 mmol, 94 mg) gave **30** as a crude mixture. The precipitate was filtrated. **30** was isolated from the precipitate using the automated flash chromatography (PuriFlash) with the PuriFlash® 12g SI-HC 15 µm (spherical silica of 15 µm) column (general procedure D). After evaporation, the counter-ion of the amidine was completely exchanged to hydrochloride following the general procedure E. The pure product was collected as a yellow solid (17.1 mg, 11%). ^{1}H NMR (400 MHz, DMSO-d_6): δ_H (ppm) 9.52 (s, 2H, NH_2), 9.16 (s, 2H, NH_2), 9.00 (s, 1H, HC=C), 8.57 (s, 1H, ArH), 8.22 (dd, J = 11.9, 8.9 Hz, 2H, ArH), 8.00 (d, J = 2.3 Hz, 1H, ArH), 7.88 (dd, J = 8.6, 1.7 Hz, 1H, ArH), 7.82 (s, 1H, ArH), 7.65 (dd, J = 8.9, 2.3 Hz, 1H, ArH), 7.42 (s, 1H, ArH), 3.95 (s, 3H, O-CH_3), 3.87 (s, 3H, O-CH_3). LC–MS (ESI) *m/z*: 435.2 (MS calcd for $C_{23}H_{19}N_2O_5S$ $[M+H]^+$, 435.1), t_R = 9.6 min, purity > 95% (UV).

1-Aminoisoquinolin-6-yl 6,7-dimethoxy-2-oxo-2H-thiochromene-3-carboxylate hydrochloride (31)

Following the general procedure C, **28b** and **36** (0.661 mmol, 130 mg) gave **31** as a crude mixture. The precipitate was filtrated. **31** was isolated from the precipitate using the

automated flash chromatography (PuriFlash) with the FlashPure EcoFlex Silica 12g column. The flow rate was 25 mL/min. The following gradient of isopropanol in acetonitrile (both modified with 0.1% formic acid) was applied: the elution started with an isopropanol/acetonitrile ratio of 40%/60% for 2 column volumes, then the ratio increased to 50%/50% over 6 column volumes, and hold for 7 column volumes. The product detection was followed by UV absorption at 254, 280, 260, 232, and 200-400 nm. The collection was threshold-based using the UV signal at 200-400 nm. The collected fractions containing the product were combined. The pure product was collected as a brown-yellow solid (26.6 mg, 9%). ^{1}H NMR (400 MHz, DMSO-*d*$_6$): δ_H (ppm) 9.15 (brs, 2H, NH_2), 9.01 (s, 1H, HC=C), 8.72 (d, J = 8.9 Hz, 1H, ArH), 7.91 (d, J = 2.1 Hz, 1H, ArH), 7.82 (s, 1H, ArH), 7.70-7.76 (m, 2H, ArH), 7.42 (s, 1H, ArH), 7.22-7.26 (m, 1H, ArH), 3.95 (s, 3H, O-CH_3), 3.86 (s, 3H O-CH_3). LC–MS (ESI) *m/z*: 409.2 (MS calcd for $C_{21}H_{17}N_2O_5S$ $[M+H]^+$, 409.1), t_R = 9.3 min, purity > 95% (UV).

6-Methoxy-isoquinoline-N-oxide hydrochloride (33)

6-Methoxyisoquinoline (**32**, 25.9 mmol, 3.75 mL) was dissolved in dichloromethane (67 mL). 3-Chloroperoxybenzoic acid (39.9 mmol, 7.18 g, 1.5 equiv) was added by portions to the stirred solution. The stirring was maintained for 3 hours. Methanol (54 mL) was added and 2/3 of solvent was evaporated under reduced pressure. 2M HCl in diethyl ether (44 mL) was added. After the addition of diethyl ether (81 mL), a precipitate was obtained, filtrated, washed with chilled diethyl ether (30 mL, 3 times), and dried to afford **31** as a white powder (5.27 g, 96%). ^{1}H NMR (500 MHz, DMSO-*d*$_6$): δ_H (ppm) 9.63 (d, J = 2.3 Hz, 1H, ArH), 8.56 (dd, J = 7.2, 2.0 Hz, 1H, ArH), 8.22 (t, J = 7.7 Hz, 2H, ArH), 7.68 (d, J = 2.3 Hz, 1H, ArH), 7.57 (dd, J = 9.2, 2.3 Hz, 1H, ArH), 3.99 (s, 3H, O-CH_3). LC–MS (ESI) *m/z*: 176.1 (MS calcld for $C_{10}H_{10}NO_2$ $[M+H]^+$, 176.1), t_R = 8.7 min, purity > 95% (UV).

1-Aminoisoquinolin-6-ol hydrochloride (36)

To a stirred solution of **33** (2.259 mmol, 478.2 mg) and *tert*-butylamine (17.13 mmol, 1.253 g, 7.6 equiv) in chloroform (22 mL), *p*-toluenesulfonic anhydride (5.718 mmol, 1.866 g, 2.5 equiv) was added by portions on ice under argon atmosphere. Stirring was maintained during one hour at 0°C. Chloroform was evaporated and the residue was dissolved in 4% $NaHCO_3$ (volume necessary to obtain pH 8). The aqueous phase was extracted by ethyl acetate (50 mL, 3 times). The organic phase was extracted by 2M HCl in water (50 mL, 8 times). The acidic aqueous phase was evaporated under reduced pressure. Methanol was added (10 mL), salts precipitated, and were discarded by filtration. The filtrate was evaporated under reduce pressure, and dried to afford the crude product **35** as a brown viscous liquid (357.6 mg). Pyridinium chloride (3.273 mmol, 378.2 mg) was added to the crude product **33**. The mixture was heated by microwave irradiation at 200°C for 2.5h. 4% $NaHCO_3$ (8 mL) was added (pH 8) and the resulting solution was diluted with water until complete dissolution. The aqueous layer was extracted by butanol (20 mL, 3 times). The organic layers were pooled, washed with brine, and the solvent was evaporated under reduced pressure. The residue was dissolved in 3M HCl in methanol (5 mL). Ethyl acetate was added (70 mL) generating a precipitate. The precipitate was filtrated, washed with ethyl acetate (10 mL), and dried to afford **36** as a brownish powder (239.4 mg, 71%). ^{1}H NMR (400 MHz, DMSO-*d*$_6$): δ_H (ppm) 8.36 (s, 1H, ArH), 8.34 (s, 2H, NH_2), 7.58 (d, J = 6.9 Hz, 1H, ArH), 7.18 (dd, J = 8.9, 2.3 Hz, 1H, ArH), 7.10 (d, J = 2.3 Hz, 1H, ArH), 6.98 (d, J = 6.9 Hz, 1H, ArH). LC–MS (ESI) *m/z*: 161.1 (MS calcld for $C_9H_9N_2O$ $[M+H]^+$, 161.1), t_R = 4.6 min, purity > 95% (UV).

N-(1-aminoisoquinolin-6-yl)-7-methoxy-2-oxo-2H-chromene-3-sulfonamide hydrochloride (42)

tert-Butyl (6-bromoisoquinolin-1-yl)(*tert*-butoxycarbonyl)carbamate (0.118 mmol, 50 mg), **41** (0.142 mmol, 36.2 mg, 1.2 equiv), K_3PO_4 (0.236 mmol, 50.2 mg, 2 equiv), and *t*BuBrettPhos Pd G3 (0.002 mmol, 2 mg, 0.02 equiv) were poured into an oven-dried flask and put under inert atmosphere. Dry toluene (307 µL) was added and the resulting solution was heated at

100°C for 72h. 2M HCl in diethyl ether (6 mL) and methanol (3 mL) were added. The solution was stirred for 48h. **42** was isolated using the automated flash chromatography (Biotage) with the FlashPure EcoFlex Silica 12g column. The flow rate was fixed at 20 mL/min. The following gradient of methanol in ethylacetate was applied: the elution started with ethyl acetate, then the methanol/ethyl acetate ratio increased to 10%/90% over 10 column volumes and hold for 3 column volumes. The product detection was followed by UV absorption at 254 and 300 nm. All fractions were collected. The fractions containing **42** were combined. After evaporation, the pure product was collected as a yellow solid (4.1 mg, 8%). ^{1}H NMR (400 MHz, DMSO-d_6): δ_H (ppm) 8.96 (s, 1H, HC=C), 8.15 (s, 1H, ArH), 8.06 (d, J = 8.9 Hz, 1H, ArH), 7.91 (d, J = 8.9 Hz, 1H, ArH), 7.64 (d, J = 6.0 Hz, 1H, ArH), 7.31 (d, J = 1.8 Hz, 1H, ArH), 7.24 (dd, J = 8.9, 2.3 Hz, 1H, ArH), 7.02-7.04 (m, 2H, ArH), 6.90 (brs, 2H, NH_2), 6.76 (d, J = 6.2 Hz, 1H, $(SO_2)NH$), 3.86 (s, 3H, O-CH_3). LC–MS (ESI) *m/z*: 398.1 (MS calcd for $C_{19}H_{16}N_3O_5S$ $[M+H]^+$, 398.1), t_R = 8.9 min, purity > 95% (UV).

Virtual fragment screening

The structure-based virtual fragment screening was achieved using Schrödinger Maestro 2019-2 software package (LLC, New York, NY). The Fragment screening compound database of Molport (Riga, Latvia) was optimized and energetically minimized via OPLS3 force field algorithm implemented in the LigPrep module of Schrödinger suite. The ionization states of the ligands at pH 7 ± 2 and the tautomers were generated by the Epik tool. The removal of the salts and the generation of all stereoisomers were then performed, leading to a maestro file including the prepared 3D structures of the fragments. The protein was prepared as previously described.[28] GLIDE v8.3 in standard precision (SP) mode docked the fragments and reported the 5000 best compounds in terms of docking score.

Chromogenic assays

The FXIIa screening assay and its data treatment were previously reported.[28,54] The FXIIa assay for confirmation and IC_{50} determination was similar; the only difference is the addition of 1 mM EDTA in the buffer. The following general procedure was used for all enzymes. Tested compounds were dissolved in DMSO and diluted to the desired concentration. The kinetic buffer consisted of 30 mM HEPES, 150 mM NaCl, and 0.005% Triton-X-100, adjusted at pH 7.4 with 1 M NaOH (5 mM $CaCl_2$ was added for thrombin and FXa assays). 6 µL of tested compound in DMSO (or DMSO alone), 10 µL of enzyme (20-fold the concentration mentioned in Table 4.S2), and 164 µL of the kinetic buffer were mixed for 5 sec and incubated for 10 min at 37°C. 20 µL of the appropriate substrate (10-fold the concentration mentioned in Table 4.S2) were then injected in each well to start the reaction. The release of *p*-nitroaniline was monitored for 3.5 minutes at 405 nm. Between each absorbance reading, the plate was shaken for 1 sec. Regarding the data treatment, the case of compounds exhibiting an IC_{50} below 10-fold the enzyme concentration was observed in this study. Therefore, an effect of the enzyme concentration was present. Because the enzyme concentration was not the same for each enzyme, the IC_{50} cannot be compared and a correction of this effect is required.[42] The apparent inhibitory constant (K_i^{app}) of tight-binding inhibitors were determined using the Morrison equation (Equation 1).[55,56]

$$v_i = v_0 \frac{[E] - [I] - K_i^{app} + \sqrt{\left([E] - [I] - K_i^{app}\right)^2 + 4[E]K_i^{app}}}{2[E]} \qquad (Eq.1)$$

where v_i is the initial reaction velocity observed at inhibitor concentration [I], v_0 is the control velocity observed in the absence of inhibitor ([I] = 0), [E] is the active enzyme concentration, and K_i^{app} is the apparent inhibition constant. The nonlinear regression was performed using GraphPad Prism 9.5.0 (730) (San Diego, CA, USA).

Intact mass protein analysis

Intact mass protein experiments were performed an Agilent 1290 Infinity II UPHLC System coupled to an Agilent 6560 IM-Q-TOF (Agilent Technologies, Santa Clara, CA, USA) with electrospray ionization (Dual Agilent Jet Stream ESI) operating in positive ion mode and an autosampler. Mass spectra were obtained using a bioZen^{TM} 3.6 µm Intact XB-C8 (2.1 x 50 mm, flow rate 0.5 mL/min, at 70°C – Phenomenex, Torrance, CA, USA) using the following gradient of the binary solvent system of mobile phase A (DMSO/water/formic acid, 3:94.5:0.5 v/v%) and mobile phase B (DMSO/isopropanol/acetonitrile/water/formic acid, 3:80:10:6.5:0.5 v/v%): 0 min, 78% of A; 0.5 min, 78% of A; 6 min, 68% of A; 7 min, 40% of A; 9 min, 40% of A. Before sample preparation, FXIIa commercial solution was buffer exchanged with 100 mM ammonium acetate pH 7 and concentrated 1.75 times using a Amicon® Ultra-0.5 Centrifugal Filter Unit (Merck KGaA, Darmstadt, Germany). The samples were prepared as follows: (1) 10 µL of 65 µM FXIIa was diluted with 14.5 µL of 100 mM ammonium acetate buffer pH 7, (2) 1 µL of 2.8 mM tested compound (or DMSO alone) was added and, after mixing, the solution was incubated for 10 min, (3) the reaction was quenched by 6 µL of 2.8% formic acid in isopropanol. 3 µL of sample was injected. Instrumental parameters were as follows: capillary voltage 4.5 kV, nozzle voltage 2 kV, nebulizer pressure 40 psi, drying gas flow 8 L/min, sheath gas temperature 300 °C, sheath gas flow 11 L/min, Quad AMU 310, acquisition rate 1.0 spectre/s, reference mass 322.048121 & 2421.91399, scan mode Standard (High Sensivity – 4GHz High resolution), and scan range 100 to 3200 *m/z*. The deconvolution was performed using the Agilent MassHunter BioConfirm Software and pMod algorithm.

Biological testing

Preparation of normal pooled plasma

The study protocol was in accordance with the Declaration of Helsinki and the recruitment of the healthy volunteers has been approved by the Ethical Committee of the CHU UCL Namur, Yvoir, Belgium (approval number: B03920096633). After a written informed consent, a total of 48 healthy volunteers were recruited at University of Namur (Namur, Belgium) in October 2021. The exclusion criteria were thrombotic and/or hemorrhagic events, antiplatelet and/or anticoagulant medication, pregnancy, and uptake of drugs that can affect the platelet and/or coagulation factor functions during the two weeks prior to the blood donation. The population study had the following characteristics: 17 males and 31 females aged from 18–57 years (mean age = 24 years) with BMI (body mass index) ranging from 16.6 – 42.1 kg.m^{-2} (mean BMI = 22.5 kg/m^2). Three and two individuals possessed the prothrombin G20210A (heterozygote) and factor V Leiden mutations, respectively. Blood was taken by venipuncture in the antecubital vein using a 21-gauge needle and collected into 0.109 M sodium citrate tubes (9:1 v/v) (Vacuette, Greiner bio-one). The supernatant fraction of blood tubes after double centrifugation for 15 min at 2500 × g at room temperature gave the platelet poor plasma. The platelet poor plasma of the 48 individuals were then pooled to obtain the normal pooled plasma (NPP). NPP was frozen at -80°C. Frozen plasma samples were thawed, heated at 25°C for 10 min, and gently mixed just before the experiment.

Activated partial thromboplastin time (aPTT) procedure

The aPTT was performed using the SynthasIL® reagent (silica activator plus phospholipids) (Werfen, Breda, Nederlands). Plasma samples were mixed with the aPTT reagent and the reaction was triggered with the addition of 20 mM $CaCl_2$, according to the manufacturer's recommendations.

Prothrombin time (PT) procedure

The PT assay was performed with the FibEx methodology, using a mixture of phospholipids (PL) and 20 pM tissue factor (TF). For the FibEx methodology[57], 80 µL of plasma samples

were mixed with 20 µL of the TF + PL. The coagulation was triggered by the addition of 20 µL of a 100 mM $CaCl_2$ solution.

Stability assays

Tested compounds were dissolved in DMSO and diluted to the desired concentration. 2 µL of tested compound in DMSO (or DMSO alone), 99 µL of PBS (without Ca^{2+} or Mg^{2+}), and 99 µL of PBS or normal pooled plasma were sealed by an adhesive aluminum foil (VWR, Leuven, Belgium) and then gently mixed for 30 min at 37°C to homogenize the solution and stabilize the temperature. The fluorescence was then recorded every 195 s for 72h (aqueous stability) or 10h (plasmatic stability) at 510 (Ex. 425), 525 (Ex. 425), and 530 (Ex. 430). Between fluorescence readings, the plate was shaken for 1 sec. The fluorescence was normalized by dividing the values with the value of the first point. The fluorescence in plasma increased over time. This effect was corrected by dividing the values with the ratio of increase of the blank. The progress curves were then fitted to the exponential one-phase decay implemented in GraphPad Prism 9.5.0 (730) (San Diego, CA, USA).

Declaration of competing interest

The authors declare no conflict of interest.

Acknowledgements

C.D. received funding from the National Fund for Scientific Research (FNRS) grant 40000455 and Fondation Léon Frédéricq grant 2020-2021-30-C.F.F. L.P. received funding from the University of Namur FSR Grant L.POCHET-12/2021. M.F. received funding from the University of Liège Fonds Spéciaux—Crédits facultaires ID 14758. We gratefully acknowledge the contribution of Oliver Garot for his technical assistance.

References

(1) Roth, G. A.; et al. Global, Regional, and National Age-Sex-Specific Mortality for 282 Causes of Death in 195 Countries and Territories, 1980–2017: A Systematic Analysis for the Global Burden of Disease Study 2017. *Lancet* **2018**, *392* (10159), 1736–1788. https://doi.org/10.1016/S0140-6736(18)32203-7.

(2) Jaffer, I. H.; Fredenburgh, J. C.; Hirsh, J.; Weitz, J. I. Medical Device-Induced Thrombosis: What Causes It and How Can We Prevent It? *J. Thromb. Haemost.* **2015**, *13* (S1), S72–S81. https://doi.org/10.1111/jth.12961.

(3) Jaffer, I. H.; Weitz, J. I. The Blood Compatibility Challenge. Part 1: Blood-Contacting Medical Devices: The Scope of the Problem. *Acta Biomater.* **2019**, *94*, 2–10. https://doi.org/10.1016/j.actbio.2019.06.021.

(4) Hong, J. K.; Gao, L.; Singh, J.; Goh, T.; Ruhoff, A. M.; Neto, C.; Waterhouse, A. Evaluating Medical Device and Material Thrombosis under Flow: Current and Emerging Technologies. *Biomater. Sci.* **2020**, *8* (21), 5824–5845. https://doi.org/10.1039/D0BM01284J.

(5) Tillman, B.; Gailani, D. Inhibition of Factors XI and XII for Prevention of Thrombosis Induced by Artificial Surfaces. *Semin. Thromb. Hemost.* **2018**, *44* (01), 060–069. https://doi.org/10.1055/s-0037-1603937.

(6) Chan, N. C.; Weitz, J. I. Antithrombotic Agents. *Circ. Res.* **2019**, *124* (3), 426–436. https://doi.org/10.1161/CIRCRESAHA.118.313155.

(7) Kalinin, D. V. Factor XII(a) Inhibitors: A Review of the Patent Literature. *Expert Opin. Ther. Pat.* **2021**, *31* (12), 1155–1176. https://doi.org/10.1080/13543776.2021.1945580.

(8) Davoine, C.; Bouckaert, C.; Fillet, M.; Pochet, L. Factor XII/XIIa Inhibitors: Their Discovery, Development, and Potential Indications. *European Journal of Medicinal Chemistry*. Elsevier Masson SAS December 15, 2020, p 112753.

https://doi.org/10.1016/j.ejmech.2020.112753.
(9) U.S. National Library of Medecine. *Safety and Efficacy Study of AB023 (Xisomab 3G3) in End Stage Renal Disease Patients on Chronic Hemodialysis*. https://clinicaltrials.gov/ct2/show/NCT03612856?term=xisomab&draw=2&rank=2 (accessed 2022-12-22).
(10) U.S. National Library of Medecine. *Xisomab 3G3 for the Prevention of Catheter-Associated Thrombosis in Patients With Cancer Receiving Chemotherapy*. https://clinicaltrials.gov/ct2/show/NCT04465760?term=xisomab&draw=2&rank=1 (accessed 2022-12-22).
(11) Mailer, R. K.; Rangaswamy, C.; Konrath, S.; Emsley, J.; Renné, T. An Update on Factor XII-Driven Vascular Inflammation. *Biochim. Biophys. Acta - Mol. Cell Res.* **2022**, *1869* (1), 119166. https://doi.org/10.1016/j.bbamcr.2021.119166.
(12) Oehmcke-Hecht, S.; Berlin, P.; Müller-Hilke, B.; Kreikemeyer, B.; Vasudevan, P.; Henze, L.; Khaimov, V.; Vollmar, B.; David, R.; Maletzki, C. The Versatile Role of the Contact System in Cardiovascular Disease, Inflammation, Sepsis and Cancer. *Biomed. Pharmacother.* **2022**, *145*, 112429. https://doi.org/10.1016/j.biopha.2021.112429.
(13) Singh, P. K.; Badimon, A.; Chen, Z.; Strickland, S.; Norris, E. H. The Contact Activation System and Vascular Factors as Alternative Targets for Alzheimer's Disease Therapy. *Res. Pract. Thromb. Haemost.* **2021**, *5* (4). https://doi.org/10.1002/rth2.12504.
(14) U.S. National Library of Medecine. *Long-term Safety and Efficacy of CSL312 (Garadacimab) in the Prophylactic Treatment of Hereditary Angioedema Attacks*. https://clinicaltrials.gov/ct2/show/NCT04739059?term=garadacimab&draw=2&rank=2 (accessed 2022-12-22).
(15) Korff, M.; Imberg, L.; Will, J. M.; Bückreiß, N.; Kalinina, S. A.; Wenzel, B. M.; Kastner, G. A.; Daniliuc, C. G.; Barth, M.; Ovsepyan, R. A.; Butov, K. R.; Humpf, H.-U.; Lehr, M.; Panteleev, M. A.; Poso, A.; Karst, U.; Steinmetzer, T.; Bendas, G.; Kalinin, D. V. Acylated 1 H -1,2,4-Triazol-5-Amines Targeting Human Coagulation Factor XIIa and Thrombin: Conventional and Microscale Synthesis, Anticoagulant Properties, and Mechanism of Action. *J. Med. Chem.* **2020**, *63* (21), 13159–13186. https://doi.org/10.1021/acs.jmedchem.0c01635.
(16) Platte, S.; Korff, M.; Imberg, L.; Balicioglu, I.; Erbacher, C.; Will, J. M.; Daniliuc, C. G.; Karst, U.; Kalinin, D. V. Microscale Parallel Synthesis of Acylated Aminotriazoles Enabling the Development of Factor XIIa and Thrombin Inhibitors. *ChemMedChem* **2021**, *16* (24), 3672–3690. https://doi.org/10.1002/cmdc.202100431.
(17) Imberg, L.; Platte, S.; Erbacher, C.; Daniliuc, C. G.; Kalinina, S. A.; Dörner, W.; Poso, A.; Karst, U.; Kalinin, D. V. Amide-Functionalized 1,2,4-Triazol-5-Amines as Covalent Inhibitors of Blood Coagulation Factor XIIa and Thrombin. *ACS Pharmacol. Transl. Sci.* **2022**, *5* (12), 1318–1347. https://doi.org/10.1021/acsptsci.2c00204.
(18) Chen, J. J. F.; Visco, D. P. Identifying Novel Factor XIIa Inhibitors with PCA-GA-SVM Developed VHTS Models. *Eur. J. Med. Chem.* **2017**, *140*, 31–41. https://doi.org/10.1016/j.ejmech.2017.08.056.
(19) Robert, S.; Bertolla, C.; Masereel, B.; Dogné, J.-M.; Pochet, L. Novel 3-Carboxamide-Coumarins as Potent and Selective FXIIa Inhibitors. *J. Med. Chem.* **2008**, *51* (11), 3077–3080. https://doi.org/10.1021/jm8002697.
(20) Bouckaert, C.; Serra, S.; Rondelet, G.; Dolušić, E.; Wouters, J.; Dogné, J.-M.; Frédérick, R.; Pochet, L. Synthesis, Evaluation and Structure-Activity Relationship of New 3-Carboxamide Coumarins as FXIIa Inhibitors. *Eur. J. Med. Chem.* **2016**, *110*, 181–194. https://doi.org/10.1016/j.ejmech.2016.01.023.
(21) Bouckaert, C.; Zhu, S.; Govers-Riemslag, J. W. P.; Depoorter, M.; Diamond, S. L.; Pochet, L. Discovery and Assessment of Water Soluble Coumarins as Inhibitors of the Coagulation Contact Pathway. *Thromb. Res.* **2017**, *157*, 126–133. https://doi.org/10.1016/j.thromres.2017.07.015.
(22) de Esch, I. J. P.; Erlanson, D. A.; Jahnke, W.; Johnson, C. N.; Walsh, L. Fragment-to-

Lead Medicinal Chemistry Publications in 2020. *J. Med. Chem.* **2022**, *65* (1), 84–99. https://doi.org/10.1021/acs.jmedchem.1c01803.
(23) Coyle, J.; Walser, R. Applied Biophysical Methods in Fragment-Based Drug Discovery. *SLAS Discov. Adv. Sci. Drug Discov.* **2020**, *25* (5), 471–490. https://doi.org/10.1177/2472555220916168.
(24) Lamoree, B.; Hubbard, R. E. Current Perspectives in Fragment-Based Lead Discovery (FBLD). *Essays Biochem.* **2017**, *61* (5), 453–464. https://doi.org/10.1042/EBC20170028.
(25) Katz, B. A.; Luong, C.; Ho, J. D.; Somoza, J. R.; Gjerstad, E.; Tang, J.; Williams, S. R.; Verner, E.; Mackman, R. L.; Young, W. B.; Sprengeler, P. A.; Chan, H.; Mortara, K.; Janc, J. W.; McGrath, M. E. Dissecting and Designing Inhibitor Selectivity Determinants at the S1 Site Using an Artificial Ala190 Protease (Ala190 UPA). *J. Mol. Biol.* **2004**, *344* (2), 527–547. https://doi.org/10.1016/j.jmb.2004.09.032.
(26) Walsh, L.; Erlanson, D. A.; de Esch, I. J. P.; Jahnke, W.; Woodhead, A.; Wren, E. Fragment-to-Lead Medicinal Chemistry Publications in 2021. *J. Med. Chem.* **2023**. https://doi.org/10.1021/acs.jmedchem.2c01827.
(27) Iversen, P. W.; Beck, B.; Chen, Y.-F.; Dere, W.; Devanarayan, V.; Eastwood, B. J.; Farmen, M. W.; Iturria, S. J.; Montrose, C.; Moore, R. A.; Weidner, J. R.; Sittampalam, G. S. HTS Assay Validation. In *Assay Guidance Manual*; 2004.
(28) Davoine, C.; Fillet, M.; Pochet, L. Capillary Electrophoresis as a Fragment Screening Tool to Cross-Validate Hits from Chromogenic Assay: Application to FXIIa. *Talanta* **2021**, *226*, 122163. https://doi.org/10.1016/j.talanta.2021.122163.
(29) MolPort. *MolPort Database*. https://www.molport.com/shop/access-databases (accessed 2023-04-18).
(30) St. Denis, J. D.; Hall, R. J.; Murray, C. W.; Heightman, T. D.; Rees, D. C. Fragment-Based Drug Discovery: Opportunities for Organic Synthesis. *RSC Med. Chem.* **2021**, *12* (3), 321–329. https://doi.org/10.1039/D0MD00375A.
(31) Rewinkel, J. B. M.; Lucas, H.; van Galen, P. J. M.; Noach, A. B. J.; van Dinther, T. G.; Rood, A. M. M.; Jenneboer, A. J. S. M.; van Boeckel, C. A. A. 1-Aminoisoquinoline as Benzamidine Isoster in the Design and Synthesis of Orally Active Thrombin Inhibitors. *Bioorg. Med. Chem. Lett.* **1999**, *9* (5), 685–690. https://doi.org/10.1016/S0960-894X(99)00069-4.
(32) Choi-Sledeski, Y. M.; Becker, M. R.; Green, D. M.; Davis, R.; Ewing, W. R.; Mason, H. J.; Ly, C.; Spada, A.; Liang, G.; Cheney, D.; Barton, J.; Chu, V.; Brown, K.; Colussi, D.; Bentley, R.; Leadley, R.; Dunwiddie, C.; Pauls, H. W. Aminoisoquinolines: Design and Synthesis of an Orally Active Benzamidine Isostere for the Inhibition of Factor XA. *Bioorg. Med. Chem. Lett.* **1999**, *9* (17), 2539–2544. https://doi.org/10.1016/S0960-894X(99)00421-7.
(33) Frédérick, R.; Robert, S.; Charlier, C.; de Ruyck, J.; Wouters, J.; Pirotte, B.; Masereel, B.; Pochet, L. 3,6-Disubstituted Coumarins as Mechanism-Based Inhibitors of Thrombin and Factor Xa. *J. Med. Chem.* **2005**, *48* (24), 7592–7603. https://doi.org/10.1021/jm050448g.
(34) Pochet, L.; Doucet, C.; Schynts, M.; Thierry, N.; Boggetto, N.; Pirotte, B.; Jiang, K. Y.; Masereel, B.; de Tullio, P.; Delarge, J.; Reboud-Ravaux, M. Esters and Amides of 6-(Chloromethyl)-2-Oxo-2 H -1-Benzopyran-3-Carboxylic Acid as Inhibitors of α-Chymotrypsin: Significance of the “Aromatic” Nature of the Novel Ester-Type Coumarin for Strong Inhibitory Activity. *J. Med. Chem.* **1996**, *39* (13), 2579–2585. https://doi.org/10.1021/jm960090b.
(35) Doucet, C.; Pochet, L.; Thierry, N.; Pirotte, B.; Delarge, J.; Reboud-Ravaux, M. 6-Substituted 2-Oxo-2 H -1-Benzopyran-3-Carboxylic Acid as a Core Structure for Specific Inhibitors of Human Leukocyte Elastase †. *J. Med. Chem.* **1999**, *42* (20), 4161–4171. https://doi.org/10.1021/jm990070k.
(36) Pochet, L.; Doucet, C.; Dive, G.; Wouters, J.; Masereel, B.; Reboud-Ravaux, M.; Pirotte, B. Coumarinic Derivatives as Mechanism-Based Inhibitors of α-Chymotrypsin and Human Leukocyte Elastase. *Bioorg. Med. Chem.* **2000**, *8* (6), 1489–1501.

https://doi.org/10.1016/S0968-0896(00)00071-7.
(37) Meth-Cohn, O.; Tarnowski, B. A Useful Synthon for Sulphur Heterocycles; I. The Synthesis of Thiocoumarins. *Synthesis (Stuttg).* **1978**, *1978* (1), 56–58. https://doi.org/10.1055/s-1978-24675.
(38) Yin, J.; Xiang, B.; Huffman, M. A.; Raab, C. E.; Davies, I. W. A General and Efficient 2-Amination of Pyridines and Quinolines. *J. Org. Chem.* **2007**, *72* (12), 4554–4557. https://doi.org/10.1021/jo070189y.
(39) Górski, B.; Basiak, D.; Talko, A.; Basak, T.; Mazurek, T.; Barbasiewicz, M. Olefination with Sulfonyl Halides and Esters: E -Selective Synthesis of Alkenes from Semistabilized Carbanion Precursors. *European J. Org. Chem.* **2018**, *2018* (15), 1774–1784. https://doi.org/10.1002/ejoc.201701766.
(40) Dar'in, D.; Kantin, G.; Kalinin, S.; Sharonova, T.; Bunev, A.; Ostapenko, G. I.; Nocentini, A.; Sharoyko, V.; Supuran, C. T.; Krasavin, M. Investigation of 3-Sulfamoyl Coumarins against Cancer-Related IX and XII Isoforms of Human Carbonic Anhydrase as Well as Cancer Cells Leads to the Discovery of 2-Oxo-2H-Benzo[h]Chromene-3-Sulfonamide – A New Caspase-Activating Proapoptotic Agent. *Eur. J. Med. Chem.* **2021**, *222*, 113589. https://doi.org/10.1016/j.ejmech.2021.113589.
(41) Hickey, S. M.; Nitschke, S. O.; Sweetman, M. J.; Sumby, C. J.; Brooks, D. A.; Plush, S. E.; Ashton, T. D. Cross-Coupling of Amide and Amide Derivatives to Umbelliferone Nonaflates: Synthesis of Coumarin Derivatives and Fluorescent Materials. *J. Org. Chem.* **2020**, *85* (12), 7986–7999. https://doi.org/10.1021/acs.joc.0c00813.
(42) Copeland, R. A. *Evaluation of Enzyme Inhibitors in Drug Discovery : A Guide for Medicinal Chemists and Pharmacologists*, Second Edi.; John Wiley & Sons: Hoboken, New Jersey, 2013.
(43) Pochet, L.; Dieu, M.; Frédérick, R.; Murray, A.-M.; Kempen, I.; Pirotte, B.; Masereel, B. Investigation of the Inhibition Mechanism of Coumarins on Chymotrypsin by Mass Spectrometry. *Tetrahedron* **2003**, *59* (25), 4557–4561. https://doi.org/10.1016/S0040-4020(03)00660-4.
(44) Pochet, L.; Frederick, R.; Masereel, B. Coumarin and Isocoumarin as Serine Protease Inhibitors. *Curr. Pharm. Des.* **2004**, *10* (30), 3781–3796. https://doi.org/10.2174/1381612043382684.
(45) Douxfils, J.; Mullier, F.; Loosen, C.; Chatelain, C.; Chatelain, B.; Dogné, J.-M. Assessment of the Impact of Rivaroxaban on Coagulation Assays: Laboratory Recommendations for the Monitoring of Rivaroxaban and Review of the Literature. *Thromb. Res.* **2012**, *130* (6), 956–966. https://doi.org/10.1016/j.thromres.2012.09.004.
(46) Koitka, M.; Höchel, J.; Gieschen, H.; Borchert, H.-H. Improving the Ex Vivo Stability of Drug Ester Compounds in Rat and Dog Serum: Inhibition of the Specific Esterases and Implications on Their Identity. *J. Pharm. Biomed. Anal.* **2010**, *51* (3), 664–678. https://doi.org/10.1016/j.jpba.2009.09.023.
(47) Breidenbach, J.; Bartz, U.; Gütschow, M. Coumarin as a Structural Component of Substrates and Probes for Serine and Cysteine Proteases. *Biochim. Biophys. Acta - Proteins Proteomics* **2020**, *1868* (9), 140445. https://doi.org/10.1016/j.bbapap.2020.140445.
(48) Wouters, J.; Huygens, M.; Pochet, L.; Pirotte, B.; Durant, F.; Masereel, B. Structural Approach of the Mechanism of Inhibition of α-Chymotrypsin by Coumarins. *Bioorg. Med. Chem. Lett.* **2002**, *12* (7), 1109–1112. https://doi.org/10.1016/S0960-894X(02)00073-2.
(49) Sandhu, H. S.; Sapra, S.; Gupta, M.; Nepali, K.; Gautam, R.; Yadav, S.; Kumar, R.; Jachak, S. M.; Chugh, M.; Gupta, M. K.; Suri, O. P.; Dhar, K. L. Synthesis and Biological Evaluation of Arylidene Analogues of Meldrum's Acid as a New Class of Antimalarial and Antioxidant Agents. *Bioorg. Med. Chem.* **2010**, *18* (15), 5626–5633. https://doi.org/10.1016/j.bmc.2010.06.033.
(50) Jiang, X.; Guo, J.; Lv, Y.; Yao, C.; Zhang, C.; Mi, Z.; Shi, Y.; Gu, J.; Zhou, T.; Bai, R.; Xie, Y. Rational Design, Synthesis and Biological Evaluation of Novel Multitargeting Anti-AD Iron Chelators with Potent MAO-B Inhibitory and Antioxidant Activity. *Bioorg.*

Med. Chem. **2020**, *28* (12), 115550. https://doi.org/10.1016/j.bmc.2020.115550.
(51) Woods, K. W.; Fischer, J. P.; Claiborne, A.; Li, T.; Thomas, S. A.; Zhu, G.-D.; Diebold, R. B.; Liu, X.; Shi, Y.; Klinghofer, V.; Han, E. K.; Guan, R.; Magnone, S. R.; Johnson, E. F.; Bouska, J. J.; Olson, A. M.; Jong, R. de; Oltersdorf, T.; Luo, Y.; Rosenberg, S. H.; Giranda, V. L.; Li, Q. Synthesis and SAR of Indazole-Pyridine Based Protein Kinase B/Akt Inhibitors. *Bioorg. Med. Chem.* **2006**, *14* (20), 6832–6846. https://doi.org/10.1016/j.bmc.2006.06.047.
(52) Armstrong, V.; Soto, O.; Valderrama, J. A.; Tapia, R. Synthesis of 3-Carboxycoumarins from O-Methoxybenzylidene Meldrum's Acid Derivatives. *Synth. Commun.* **1988**, *18* (7), 717–725. https://doi.org/10.1080/00397918808077361.
(53) Li, M.; Petersen, J. L.; Hoover, J. M. Silver-Mediated Oxidative Decarboxylative Trifluoromethylthiolation of Coumarin-3-Carboxylic Acids. *Org. Lett.* **2017**, *19* (3), 638–641. https://doi.org/10.1021/acs.orglett.6b03806.
(54) Davoine, C.; Pardo, A.; Pochet, L.; Fillet, M. Fragment Hit Discovery and Binding Site Characterization by Indirect Affinity Capillary Electrophoresis: Application to Factor XIIa. *Anal. Chem.* **2021**, *93* (44), 14802–14809. https://doi.org/10.1021/acs.analchem.1c03611.
(55) Kuzmič, P.; Elrod, K. C.; Cregar, L. M.; Sideris, S.; Rai, R.; Janc, J. W. High-Throughput Screening of Enzyme Inhibitors: Simultaneous Determination of Tight-Binding Inhibition Constants and Enzyme Concentration. *Anal. Biochem.* **2000**, *286* (1), 45–50. https://doi.org/10.1006/abio.2000.4685.
(56) Schwartz, P. A.; Kuzmic, P.; Solowiej, J.; Bergqvist, S.; Bolanos, B.; Almaden, C.; Nagata, A.; Ryan, K.; Feng, J.; Dalvie, D.; Kath, J. C.; Xu, M.; Wani, R.; Murray, B. W. Covalent EGFR Inhibitor Analysis Reveals Importance of Reversible Interactions to Potency and Mechanisms of Drug Resistance. *Proc. Natl. Acad. Sci.* **2014**, *111* (1), 173–178. https://doi.org/10.1073/pnas.1313733111.
(57) Evrard, J.; Siriez, R.; Bouvy, C.; Favresse, J.; Yildiz, H.; Hainaut, P.; Mullier, F.; Dogné, J.; Douxfils, J. Comparison of Analytical Performances between Clot Waveform Analysis and FibWave in Edoxaban-treated Patients and Healthy Controls. *Res. Pract. Thromb. Haemost.* **2022**, *6* (7), e12804. https://doi.org/10.1002/rth2.12804.